ChemCatChem

Review
doi.org/10.1002/cctc.202301672

Chemistry Europe
European Chemical Societies Publishing

www.chemcatchem.org

Transition Metal Catalysts for the Glycerol Reduction: Recent Advances

Francesca Coccia,[a] Nicola d'Alessandro,[b, c] Andrea Mascitti,[b] Evelina Colacino,[d] and Lucia Tonucci*[a]

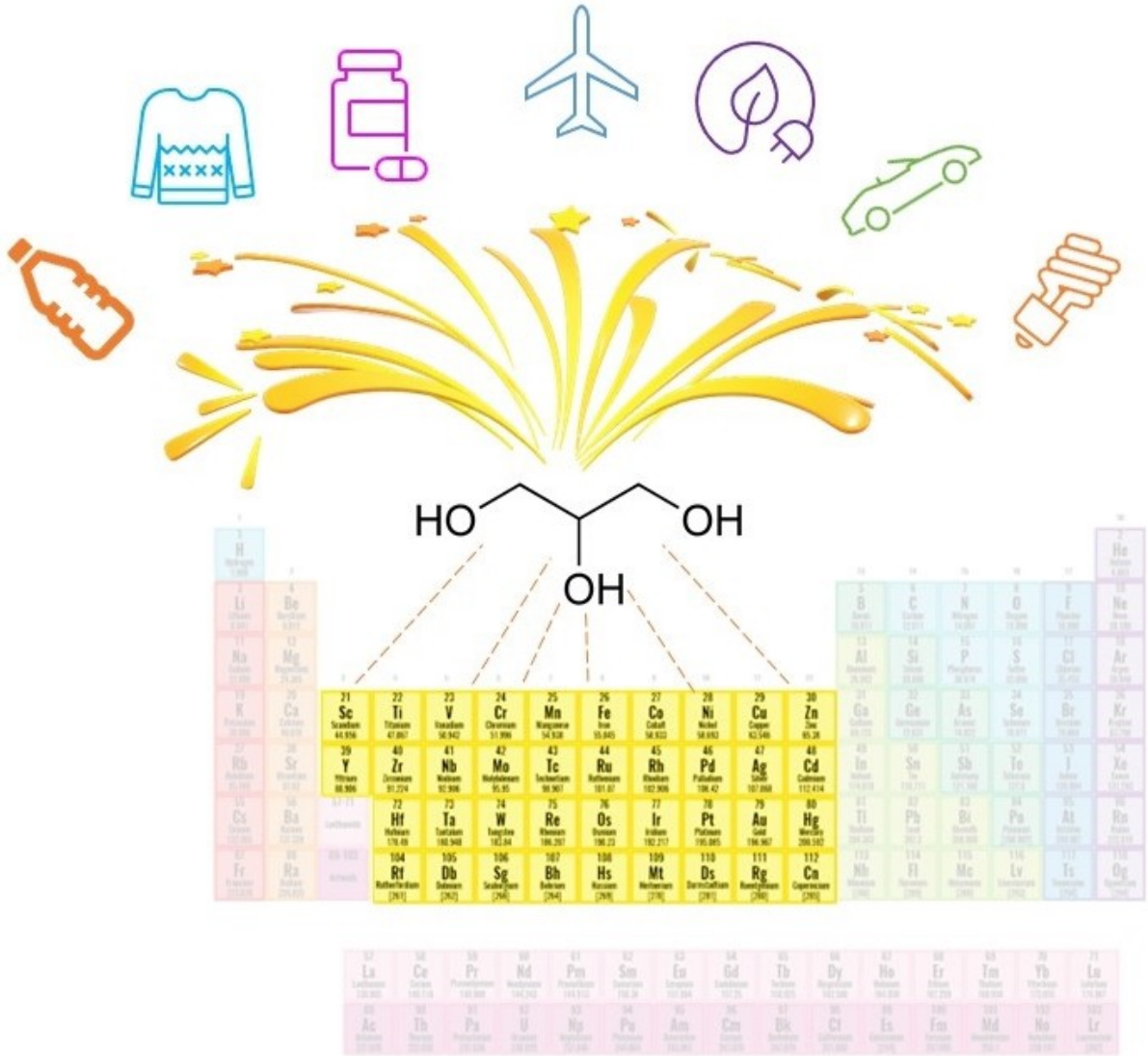

Glycerol (GL) represents a widespread agro-industrial waste. Its valorization is pivotal for a sustainable society because GL is a renewable compound deriving from biomass, but it has a high oxygen to carbon ratio, compared with feedstock used in the energy and chemistry sectors. Oxygen-poor derivatives are easily and immediately transferable to the industry, avoiding a deep and pressing modification of the plants. From this perspective, keeping the carbon content but with an oxygen content reduction, we could effectively obtain the enhancement of the recovery and the use of GL converting it into attractive industrial building-blocks. In this Review, we present and discuss the up-to-date results about the chemical reduction of GL into products with 3 carbon and 0, 1, or 2 oxygen atoms. The focus is on the transition metal (TM) catalysts that have made the hydrogenation reactions of GL possible, partitioning the metals into early and late, based on their position in the periodic table. This discussion will contribute to select and develop new catalysts aimed at the improvement of the yield and of the selectivity in the hydrogenation reactions of GL.

1. Introduction

The energy transition represents the passage from a society based on an energy mix centered on fossil fuels to one with low or zero carbon emissions, better if based on renewable resources. In recent years, the topic of decarbonization has been given serious consideration, specifically for the electrification of consumption, which involves replacing electricity produced from fossil fuels with electricity generated from renewable sources. This challenge will be the greatest of the entire century; therefore the total replacement of carbonaceous resources (*e.g.*, with hydrogen) will certainly contribute to the decarbonization of our Planet, but, in a short time, it will also be necessary to associate other strategies to change not the materials for energy use but simply their origin.[1] For example, ethanol can be obtained from ethene by catalyzed hydration reaction or even by sugar fermentation. Its synthetic catalytic production decreased significantly since the 1980s until a value of 7% in 2010[2] due to the increase in the prices of fossil resources and also to the change of approach to environmental sustainability and renewable feedstocks. At the same time, the fermentative pathway from sugars, starchy and lignocellulosic materials, better if available as wastes, noticeably increased. Moreover, it has recently been proposed the reverse synthetic hydration reaction able to furnish polyethylene starting from the catalytic dehydration of bioethanol.[3]

Generically, a large part of industrial carbonious waste is polar compounds with relatively high oxygen to carbon ratio (O/C), at least compared with similar materials used for energy purposes. Green Chemistry Principles, and particularly the number 2 (atom economy), impose to save any atom when passing from reagents to products; however, losing carbon or oxygen atoms is not the same, since oxygen is ubiquitously available. On the other hand, oxygen-poor derivatives will be much more eligible for actual and future industrial applications. Therefore, we can propose an innovative perspective that aims to achieve less polar compounds from any feedstocks keeping selectively the carbon content and reducing the oxygen content (Figure 1).

To reach this goal, several strategies were applied. Thermal processes are widely diffused, often assisted by homogeneous or heterogeneous catalysts.[4] Liquid biomasses like vegetable oils, as such or after a hydrolytic step to free fatty acids, were successfully deoxygenated to form hydrocarbons by using, for example, a γ-alumina supported Ni/Mo catalyst, at 300–400 °C, in H_2 atmosphere.[5,6] More recently even biomass of different nature, like lignocellulosic materials, were subjected to controlled oxygen removal to obtain a series of functional high-value low-oxygenated olefins or hydrocarbons.[7,8] Several contributions on rhenium catalyzed deoxydehydration reaction (DODH, formal removal of a H_2O_2 unit from a diol) appeared recently in literature (Scheme 1).

[a] *Dr. F. Coccia, Dr. L. Tonucci*
Department of Philosophical, Educational and Economic Sciences
University "G. d'Annunzio" of Chieti-Pescara
Via dei Vestini, 66100 Chieti, Italy
E-mail: lucia.tonucci@unich.it

[b] *Prof. N. d'Alessandro, Dr. A. Mascitti*
Department of Engineering and Geology
University "G. d'Annunzio" of Chieti-Pescara
Via dei Vestini, 66100 Chieti, Italy

[c] *Prof. N. d'Alessandro*
UdA-TechLab, Research Center
University "G. d'Annunzio" of Chieti-Pescara
66100 Chieti, Italy

[d] *Prof. Dr. E. Colacino*
ICGM, Univ Montpellier, CNRS, ENSCM
Montpellier 34296, France

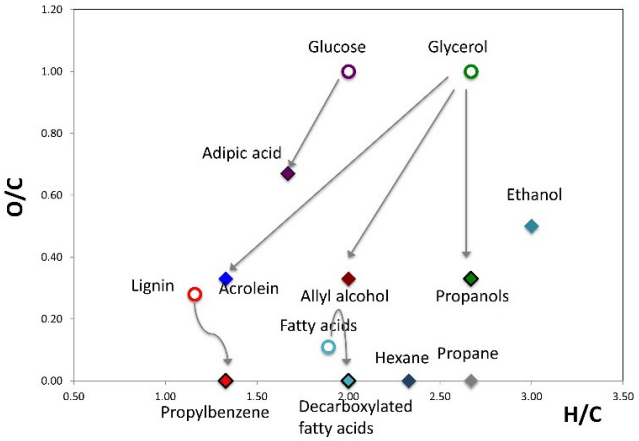

Figure 1. The correlation between the number of O and the number of H atoms, per C atom, in selected organic compounds deriving from biomass.

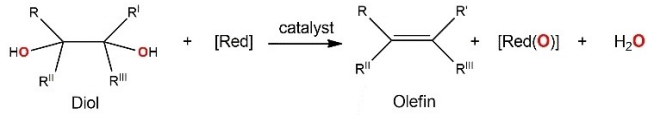

Scheme 1. Catalyzed DODH reaction of a diol to obtain its olefin derivative.

The value of this reaction is that many natural polyols, often available as waste, can be transformed into low oxygenated derivatives (or even hydrocarbons) useful as monomers in the polymer industry, as fuel or as building-blocks.[9,10]

In this review, we have focused our attention just to the smallest natural polyol, widespread in nature, since it is a primary constituent of lipids. Glycerol (GL) molecule is the second simplest sugar alcohol and the first available in considerable amounts in nature. However, we are strongly convinced that the remarks of this review can be applied also to other important natural sugar alcohols with a more complex structure, like erythritol, xylitol or sorbitol.

As for ethanol, even for GL, its release on the world market changed during the last fifty years. It is obtained mainly from two routes: i) *via* petrochemical sources (synthetic GL) or ii) as a by-product of oleochemical production (bioglycerol). Regarding its industrial availability, the transition from the i) to the ii) route occurred about the 2000s when biodiesel started to be introduced massively on the market to replace part of the fossil diesel fuel, so making available a large amount of bioglycerol, equivalent to about 10% w/w of the transesterified lipids. This abundance, other than to contribute suppressing almost totally the synthetic route from propene, prompted the industries to reverse the former Solvay technology, and transform it to a

Francesca Coccia, M.Sc. in Chemistry and Pharmaceutical Technologies, received her Ph.D. in Chemical Sciences from University "G. d'Annunzio" of Chieti-Pescara (Italy), then she moved to Milan University (Italy) in the Benaglia group, working about the organic catalysts supported on different materials. In 2018 she started a postdoc position in CNR (National Research Council) of Macromolecules at Milan for the functionalization of natural polymers; now she is Assistant Professor of Inorganic Chemistry at the University "G. d'Annunzio" of Chieti-Pescara. Her research focuses on materials functionalization, Green Chemistry and catalysis by metal nanoparticles.

Nicola d'Alessandro obtained his Ph.D. in Chemistry at the Photochemistry Research Group of University of Pavia (Italy), studying the photochemical reaction between aromatic nitriles and benzylic donors. He then joined the Mariano Research group at the University of Maryland (US) and the von Sonntag Research Group at the Max Planck Institute für Strahlenchemie (Mulheim, Germany). After a brief experience at the University of Torino (Italy), in 1997 he moved to the University "G. d'Annunzio" of Chieti-Pescara (Italy) where, since 2005, he is Chemistry Associate Professor. His main research activity concerns the chemical transformations of widely-available agro-by-products catalyzed by transition metals.

Andrea Mascitti, M. Sc. in Chemistry and Advanced Chemical Methodologies at University of Camerino (Italy), received his Ph.D. in Biomolecular and Pharmaceutical Sciences from University "G. d'Annunzio" of Chieti-Pescara (Italy) where he is now a Research fellow. His research focuses on Green Chemistry, the valorization of agro-industrial waste and metal catalysis.

Evelina Colacino received her double Ph.D. (with European Label) in 2002 at the University of Montpellier II (France) and the University of Calabria (Italy). Associate Professor of Organic Chemistry at the University of Montpellier (France), she promotes sustainability in Higher Education by integrating green chemistry in academic curricula, with a special focus on the fundamentals and the practice of mechanochemistry. Her main research activities concern the development of sustainable approaches by mechanochemistry to prepare value-added compounds for the industry, with a special focus on Active Pharmaceutical Ingredients. Green catalytic methods in non-conventional media using enabling technologies are also explored. She chairs of the European Programme COST Action CA18112 MechSustInd (Mechanochemistry for Sustainable Industry) and the Horizon Europe Project IMPACTIVE (Innovative Mechanochemical Processes to synthesise green ACTIVE pharmaceutical ingredients)

Lucia Tonucci, M.Sc. in Chemistry at University of Bologna (Italy), received her Ph.D. in Chemical Sciences at University "G. d'Annunzio" of Chieti-Pescara (Italy) where she is now Assistant Professor of Inorganic Chemistry. She is the Academic Coordinator for Public Engagement at the University "G. d'Annunzio" and is engaged in the dissemination about Green and Sustainable Chemistry, and Science and Society. Her research focuses on the Green Chemistry and the valorization of agro-industrial waste by metal catalysts and photocatalysts for chemistry and energy sectors.

method to obtain green epichlorohydrin from natural GL (Epicerol technology; Solvay first and Technip Energies subsequently).[11] In 2018–2022, the annual global production of crude GL was around 6 Mton;[12] the major contribute comes from biodiesel industry (60%), increasing to 80% in EU production with an amount of 1 Mton.[13]

Within this review, deoxygenated GL products, such as a series of C_3 compounds having 0, 1, or 2 oxygen atoms (Figure 2), crucial as green industrial feedstocks, will be considered and the TM-catalyzed technologies able to obtain them from GL, published from 2017 on will be described. We stated that 2-hydroxypropanal, glycidol and propanoic acid were not reported as significative products from GL chemical reductions, at least in this time range. So, we don't cite them in this review.

The presence of a catalyst is mandatory for deoxygenation reactions on polyols. Excluding the biodeoxygenation reactions, it remains to consider the TMs as the unique candidates to perform green and sustainable catalytic procedures. TM examined and named in the paragraph titles of this review are only those reported in scientific literature as effective catalysts for the deoxygenation reactions of GL to C_3 products, at least in the time interval in question. TMs are characterized by partially filled *d* orbital subshells in the free elements and, for most of them, also for their cations. Unlike the main group elements, the TMs also exhibit horizontal chemical similarities. Electronegativity increases from left to right and from top to bottom, making differently reactive the left side (early) and right side (late) elements. The review is organized, comparing these two groupings, to answer a crucial question: "What is the reason for late TMs being used more frequently? Is it because of their peculiar reactivity, mainly due to their electronic properties, or, simply, because some metals, extensively used in the past, continue to be used along well-standardized paths rather than testing new solutions with the risk of having major failures?"

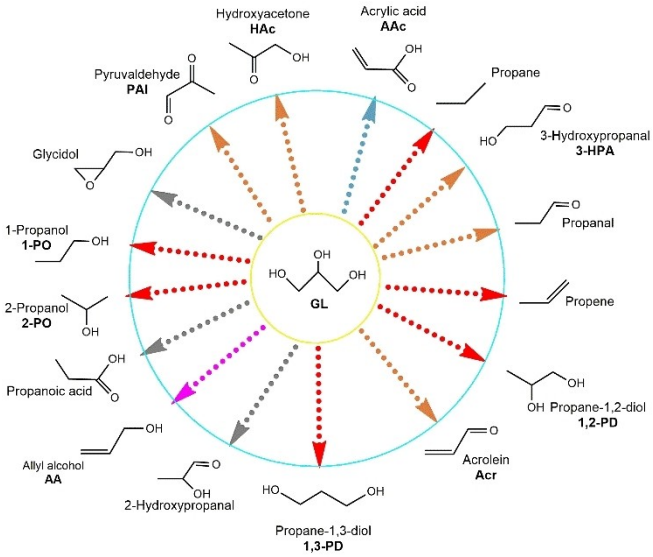

Figure 2. C_3 compounds from the deoxygenation of GL, considered in this review. The color of the arrows reflects the main reaction pathways to the product: red, hydrogenolysis; green, oxydehydration; pink, deoxydehydration; orange, dehydration; grey, not present in literature in the range time.

2. Early Transition Metals

2.1. Titanium

In the large world of GL deoxygenation reactions, titanium (Ti sponge average price: 7.26 $/kg)[14] has been used mostly as active support.[15] The success of titanium oxide is due to its acidity since Lewis Acid sites (LAS) are needed for the C–O cleavages in the dehydration reactions; however, too many of these sites could also promote C–C cleavage through an acidic cracking mechanism.[16] Villa *et al.* reported the counter proof of this evidence: bimetallic Au-Pt catalysts were tested in the GL hydrogenolysis, using oxide supports with different acid–base properties (such as TiO_2 and MgO).[17] The medium strength of TiO_2 LAS led to the best performance in terms of activity, stability of the catalytic system and selectivity towards propane-1,2-diol (1,2-PD), avoiding the formation of ethanol, methanol or propanols by over-hydrogenolysis of 1,2-PD.[17]

Diols, such as 1,2-PD and propane-1,3-diol (1,3-PD), are useful products, largely employed in polymer industries (*e.g.*, packaging, fiber, filler) that can be obtained by hydrogenolysis of GL.[18,19] The reaction is a variegated process that can be conducted, for example, on a metal-acid bifunctional catalyst, able to promote dehydration, *via* intermediates as hydroxyacetone (Hac) and 3-hydroxypropanal (3-HPA), followed by a hydrogenation reaction occurring on metal sites.[19]

It was observed that increased aqueous GL conversion (from 53% to 74%) and 1,3-PD yield (from 20% to 25%) were obtained if TiO_2 was used as support for $Pt/WO_3–ZrO_2$ catalyst, carrying out the reaction in a vertical stainless steel fixed-bed reactor at 523 K and 50 bar H_2 pressure.[20] An explanation of this improvement could be the introduction of TiO_2 that increased the Brønsted acidity of the catalyst: WO_x species were linked, through O bridges, to Zr but also to Ti, with a larger electronegativity than Zr. It was noted a linear correlation between the 1,3-PD yield and the concentration of the Brønsted acid site (BAS) and the 1,2-PD yield and the amount of LAS. In this case, the generation of *in situ*-BAS could be explained with the H_2 dissociation on the Pt surface forming $H^{\cdot}$ atoms and then, during $H^{\cdot}$ spillover, the electron-donation from $H^{\cdot}$ to the LAS of the support produced H^+.[20] Even other parameters, such as properties of Pt and of the supports, can affect the generation of BAS. Besides these aspects, also the temperature can play an important role, especially in increasing the GL conversion. Moreover, when Pt loading was augmented from 1% to 3%, the GL conversion raised, but the selectivity of the reaction changed, leading to 1-propanol (1-PO) instead, while with a Pt loading of more than 4%, the substrate transformation decreased, due to the aggregation of Pt particles.[20] The morphology of the TiO_2 support affected the conversion and the selectivity: using rutile to obtain a $Pt-WO_x/TiO_2$, a high conversion was observed (81%) with an acceptable 1,3-PD selectivity (51%) but, using anatase, only 7% of GL was

converted mainly to 1-PO (62% selectivity).[21] Using hollow mesoporous SiO_2-TiO_2 nanosphere catalysts, it was possible to load and distribute Pt nanoparticles and WO_x nanoclusters very well into the solid support structure.[22] This $Pt/WO_x/SiO_2$-TiO_2 fully catalyzed the GL conversion (85%), with a high 1,3-PD selectivity (54%) at 423 K and 40 bar H_2 pressure. During the recycle tests, the selectivity slightly decreased because of the over-hydrogenolysis to 1-PO. It is possible also to dope Pt/TiO_2 with Cr, Mo or W oxides to tune the products of hydrogenolysis at 513 K and 30 bar H_2: in the presence of Cr and Mo, the main product was 1,2-PD (80% and 60%, selectivity); with W, 1,3-PD was obtained with 50% selectivity.[23]

TiO_2 was used as a support for the deoxygenation of GL using Cu-based catalysts. The results were compared with those obtained in the presence of more acidic support such as Al_2O_3.[24] The catalytic activity of Cu/TiO_2 and Cu/Al_2O_3 catalysts led to the same conversion; however, the selectivity was different. In particular, Cu/Al_2O_3 catalyst was more selective to 1,2-PD and HAc compared Cu/TiO_2, mainly leading to 1-PO. The addition of NaOH (5 wt%) in the reaction mixture with Cu/TiO_2 increased the selectivity for 1,2-PD to 92%, with 52% of GL conversion (at 473 K and 40 bar H_2), since the presence of hydroxide ion promoted the dehydration of glyceraldehyde, formed by dehydrogenation of GL, giving 2-hydroxyacrolein as intermediate compound (Scheme 2).[24]

Recently, monometallic Cu/γ-Al_2O_3 or Cu/TiO_2 catalysts were reported to be able to significantly increase the reaction selectivity towards the formation of HAc, at 553 K in gas phase and atmospheric pressure under N_2. The results confirmed that this reaction was catalyzed by both the metal and by acid sites of the solid support.[25] In particular, 50% of HAc and 20% of pyruvaldehyde (PAl) selectivities were obtained over Cu/TiO_2 catalyst, at a lower extent compared to Cu/γ-Al_2O_3 catalyst (70% and 40%, respectively). The reason for this outcome relies on the nature of the support: indeed, TiO_2, presents both acidic and basic sites, differently than this home-made alumina, which presents very strong acid sites. However, both catalysts suffered from deactivation, caused by the copper oxidation. The reactivation was feasible by thermal treatment at 723 K, followed by a reduction step with H_2/Ar.[25]

A high performance of TiO_2 used as support in GL dehydration was evidenced even by Ginjupalli *et al.* They synthesized tungstate metal phosphate (WO_x/MP; M = Al, Zr, Ti) solid supported acid catalysts for vapor phase GL dehydration to acrolein (Acr) and HAc operating at 593 K, under atmospheric pressure in a vertical fixed-bed quartz reactor. Their outcomes (100% GL conversion and 80% Acr selectivity) demonstrated that WO_x/TiP was the most selective and stable catalyst (compared to those supported on AlP or ZrP) owing to the acceptable amount of surface acidity and the substantial number of pores available on its surface.[26] By DFT (Density Functional Theory) calculation, it was demonstrated that the adsorption through the central hydroxyl group of GL on the TiO_2 anatase surface had the best geometry and energy (−30.91 kcal/mol) to promote the dehydration reaction leading to Acr.[27] Dehydration of GL to Acr was also studied over the widely used Keggin-type heteropolyacids (*i.e.*, $H_4SiW_{12}O_{40}xH_2O$ and $H_4PVMo_{11}O_{40}xH_2O$) supported on several metal oxides (TiO_2, Al_2O_3, ZrO_2, AlTiZr oxide).[28] TiO_2 resulted the best support for the active $H_4SiW_{12}O_{40}$: Acr was obtained selectively at 498 K by complete conversion of aqueous GL.[28]

The good dispersion of nano-size metal particles on titania surface represents an additional advantage to its use, as demonstrated by investigating GL conversion and selectivity to propanols, 1-PO + 2-PO (2-propanol), at 493 K and atmospheric pressure, as a function of metal phosphate supported platinum catalysts (Pt/AlP, Pt/TiP, Pt/ZrP and Pt/NbP).[29] Among all catalysts investigated, Pt/TiP showed a significant catalytic performance in one-step vapor phase hydrogenolysis of GL to propanols (100% conversion of GL and 97% selectivity for propanols, 1-PO 87% and 2-PO 10%). The authors reported that the activity of this catalyst was due to its acidity and to the good dispersion of platinum particles on the TiO_2 surface. The catalyst was reusable only one time with a weak decay in its catalytic activity.[29]

The use of TiO_2 as support fostering the activity of the catalyst is valuable in the perspective of reducing the amount of expensive critical raw materials, usually needed for this transformation. For example, iridium nanoparticles stabilized over modified ReO_x on rutile TiO_2 were effective for the GL hydrogenolysis to 1,3-PD (67% selectivity with 35% conversion).[30] Although the support was not directly involved in the reaction mechanism, it joined to stabilize and to uniformly disperse the Ir nanoparticles and to favor the contact between the Ir species and ReO_x.[30]

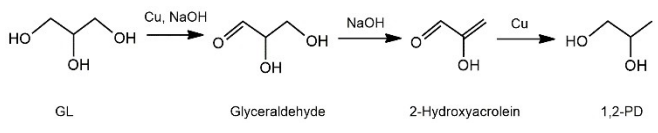

Scheme 2. Mechanism of GL hydrogenolysis and dehydration of glyceraldehyde under basic conditions.

2.2. Vanadium

Vanadium (average market price: 176.16 $/kg)[31] is the 20th most abundant element in the Earth's crust and the 6th one among the TMs.[32] In aqueous solution, the most accessible oxidation states range from +2 (d^3) to +5 (d^0); therefore, V^{II} compounds could act as reducing agents, while V^{V} compounds as oxidizing agents.[33] The vanadium affinity for oxygen leads to passivation of the metal surface in air; this characteristic enhances the catalyst activity and selectivity towards the oxidation reaction step.[34] It is noteworthy that several selective oxygen transfer reactions in the presence of vanadium complexes were reported,[35] also with polyoxometalates.[36]

Acrylic acid (AAc) is produced mostly by propene oxidation in industrial synthesis, and Acr constitutes a transient compound.[34] From a green perspective, GL oxydehydration could be a competitive route with that from petrochemicals to obtain AAc, a key compound for the polymer industry: plastics, fibers, paints, polishes, coatings, and adhesives.[37] The use of a

catalyst with BAS allows to dehydrate GL to 3-HPA and Acr first, subsequently oxidized to AAc in the presence of the metal sites of the catalyst having mild oxidative capability (Scheme 3). Chieregato *et al.* suggested that even the presence of LAS is a very important factor contributing to the oxidation step of Acr, making possible its coordination with the nucleophilic oxygen species (*i.e.*, O^{2-}) present on the surface and generated by V ions, likely V^{5+}.[38]

Vanadium oxide catalysts constitute the right compromise because they are sufficiently acidic to catalyze the dehydration step, but not so acidic to inhibit the desorption of AAc.[38] On the contrary, the presence of highly active redox-metals, such as noble metals, could cause direct oxidation of GL and decomposition of Acr to CO_x rather than the controlled oxidation to AAc (Scheme 4).[39,40]

Mixed $Mo_xV_yO_z$ oxides, supported on acidic ZSM-5 zeolite, were able to produce AAc from GL, with low coke deposition and high stability of the catalyst.[41]

The dehydration of GL to Acr, in the presence of solid acid catalysts, is generally viable but, in several cases, their deactivation, due to coke deposition, remains a huge barrier. However, the transformation of GL to Acr and AAc was investigated at 573 K, using mixed vanadium and molybdenum oxides supported on alumina.[42] Their catalytic activity was recovered due to the vanadium mediated degradation of coke. Recently, a Keggin-type vanadium-substituted phosphomolybdic acid supported on mesoporous MCM-41 was reported for the catalytic dehydration of GL to Acr in a fixed-bed tubular reactor at 498 K and 1 bar of pressure, under N_2 flux. The authors observed that the Acr selectivity depended on the vanadium-substituted phosphomolybdic acid loading. The selectivity raised to 68% increasing the amount of vanadium phosphomolybdic acid to 40%, which also enhances BAS, suggesting that the selectivity of the reaction to Acr depends on the Brønsted acidity.[43]

Mo–V mixed oxides were hydrothermally synthesized in the presence of ionic surfactants (*i.e.*, sodium dodecyl sulfate and cetyltrimethylammonium bromide) which led to the formation of nanorod-type crystals.[44] This peculiar morphology favored the redox process bringing better catalyst performance. The catalysts produced with both surfactants presented higher productivity of AAc and good catalytic stability compared to the reference catalyst prepared without surfactants, with no coke formation and a considerable decrease in CO_x evolution during 6 h of reaction (from 66% to 36%). The catalyst synthesized in the presence of sodium dodecyl sulfate showed the best catalytic results with 100% of conversion and 57% of AAc selectivity at 593 K and atmospheric pressure in a fixed-bed reactor.[44] Vieira *et al.* achieved a one-pot oxydehydration of GL (AAc selectivity was about 46%) in the presence of 3D and 2D vanadosilicates, with structures similar to ferrierite and ITQ-6 zeolites, but without framework aluminum.[45]

A vanadium catalyst (NH_4VO_3) was used to catalyze GL DODH producing 22% allyl alcohol (AA) and small amounts of Acr (Scheme 5) and propanal.[46] This catalyst afforded yield and selectivity comparable to the methyltrioxorhenium (MTO) in the same reaction conditions, under 1 H_2 bar pressure at 548 K in neat GL.[46]

Silicates modified with vanadium and niobium were also tested at 523 K using H_2O_2 as an oxidizing agent for the dehydration/oxidation of GL. The catalytic test showed GL conversion up to 95% with good selectivity to AA (if commercial GL is used) or acetone (if waste GL is used).[47] The catalysts assumed a needle morphology, with small particle size (two distributions: 55 and 160 nm) raising the amount of exposed niobium.[47] Almeida *et al.* supported vanadium oxide on beta zeolite (Si/Al = 25 with 4% V) and used it for the one-pass gas-phase conversion of GL to AA without any external reductant.[48] The presence of zeolite allowed the dehydration to Acr thanks to its acid sites. Carrying out the reaction at 593 K under atmospheric pressure, in a fixed-bed flow type quartz reactor, it was possible to reach a 30% of selectivity for AA with a 20% of GL conversion. Modifying the acidity of the vanadium beta-zeolite, it was possible to address the conversion to the AA and AAc which resulted favored by a low acidity density and the presence of redox sites; a high presence of acid sites promoted a dehydration of GL to Acr.[49,50]

Another example of flow equipment was used for gaseous GL direct conversion to AA without any sacrificial additive.[51] Porous MoFe/x-KIT-6 (x = V, Nb, or Ti) oxide catalysts with high specific surface area were prepared, through *in situ* hydrothermal and wet impregnation methods. At 613 K under atmospheric pressure, all the catalysts showed high activity in

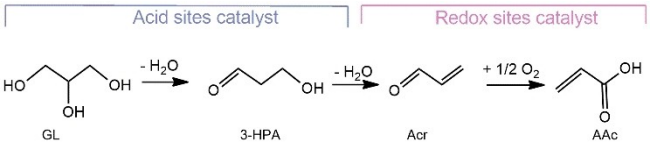

Scheme 3. Oxydehydration reaction pathway of GL to AAc.

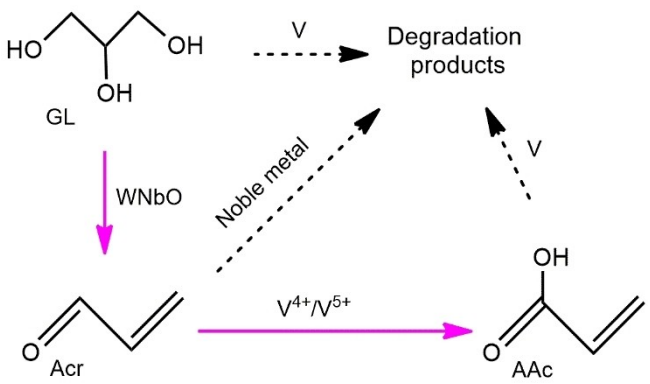

Scheme 4. The direct oxidative dehydration of GL over WVNbO catalyst to Acr e AAc.

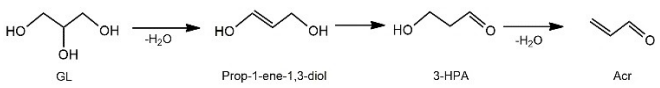

Scheme 5. The proposed catalyzed mechanism for the catalyzed formation of Acr.

the gaseous GL catalytic conversion with AA (31% yield), Acr (17%) and acetaldehyde (13%) as the main products.[51]

Among all catalysts, MoFe/V-KIT-6 showed improved catalytic stability and good regeneration performance besides higher GL conversion (92%) and AA selectivity (31%), while the total selectivity of AA, Acr, acetaldehyde and HAc reached about 70%. The reasons for this success could be ascribed to the strong interactions between the V-KIT-6 and MoFe oxides reducing the surface acid density, as well as providing the ordered mesoporous structure.[51]

In Table 1 a summary of the V-based catalysts, reported in vanadium paragraph, and their selectivity in AAc, Acr and AA were reported.

2.3. Chromium

Chromium is the 7th most abundant element on Earth (average market price: 9.794 $/kg),[52] most of it resides in the core and mantle.[53] it's a common groundwater and soil contaminant, particularly in industrial areas, and is listed by the US Environmental Protection Agency as one of 129 priority pollutants.[54] There are few research works in the literature of last years about the use of chromium in catalyzed GL conversion to C_3 deoxygenated compounds, probably due to its toxicity. In 2017 the adsorption, configurations and energetics of the reactants, intermediates and final products of the GL hydrogenolysis on metallic Cu were studied and compared with spinel $CuCr_2O_4$, by DFT experiments.[55] They observed that the formation of HAc (by cleavage of the terminal hydroxyl group), as intermediate, is thermodynamically and kinetically favored to that of 3-HPA (by cleavage of the central hydroxyl group), for both catalysts, leading to 1,2-PD as main reaction product (Scheme 6). The Cu species are the real active catalyst for the C–O cleavage, whereas the Cr atom gives to GL a stable adsorption site to facilitate C–O cleavage by the copper in the dehydration step, that is the rate-limiting step. The dehydration path from GL to HAc (upper in Scheme 6) resulted thermodynamically and kinetically favorite in these conditions. The hydrogenation of HAc to 1,2-PD on the $CuCr_2O_4$ surface is thermodynamically and kinetically more favored than that on the Cu surface, thanks to the formation of bonds between Cr and oxygens, and the formation of hydrogen bonds stabilizes the transition states. These data were supported by experimental results of the reaction carried out under 40 bar H_2 and at 493 K for 12 h in water solution. The authors declared 32% of GL conversion and a 1,2-PD yield of 24%.[55]

Recently, chromium silicates with MFI structure were tested as heterogeneous catalysts for gaseous GL conversion into acetaldehyde and Acr as main products. The reaction was performed at 773 K under atmospheric pressure in a continuous-flow glass fixed-bed reactor, leading to high GL conversion (97%) to acetaldehyde and Acr in a 30% and 10% yield, respectively.[56]

Table 1. Vanadium catalysts in the hydrogenation of GL.

Catalyst	Main Product	Selectivity (mol%)	Ref.
Mo-V mixed oxides with ionic surfactants	AAc	57	[44]
Vanadosilicates	AAc	46	[45]
$Mo_xV_yO_z$ oxides on acidic ZSM-5	AAc Acr	18 28	[41]
V_2MoO_8 on alumina	Acr	75	[42]
Vanadium-substituted phosphomolybdic acid on mesoporous MCM-41	Acr	68	[43]
VO_x on beta zeolite	AA	30	[48]
VO_x on beta zeolite	AAc	46	[50]
Porous MoFe/x-KIT-6 (x = V, Nb, or Ti) oxide	AA	31	[51]
NH_4VO_3	AA	22	[46]
Vanadium-niobium silicates	AA	14	[47]

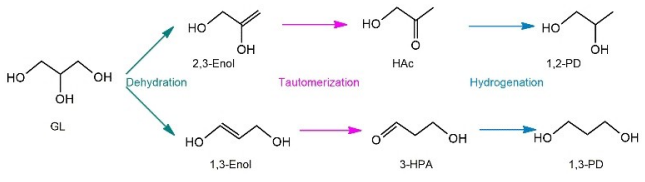

Scheme 6. The potential dehydration–hydrogenation mechanisms of GL hydrogenolysis; in the presence of spinel $CuCr_2O_4$, the upper pathway is thermodynamically and kinetically favored. Adapted with permission from Y. S. Yun, T. Y. Kim, D. Yun, K. R. Lee, J. W. Han, J. Yi, *ChemSusChem* 2017, 10, 442–454. Copyright 2017 John Wiley and Sons.

2.4. Zirconium

An approach to make the sustainable reactions more suitable for industrial applications is to carry out them in flow mode, using supported catalysts.[57] This approach allows to reuse the catalyst and avoids metal leaching into the reaction medium. Performing the reaction in a fixed-bed reactor is a guarantee of safety, especially if hazardous reagents are employed, such as H_2, used in many studies of GL deoxygenation. Performing the reaction in very small channels of a reactor or microreactor, the consumption (amount) of these dangerous reagents is very low per minute and so the chemical risk decreased. The possibility to carry out the reaction in continuum, feeding the reactor with a mixture of reagents (without catalyst) through a syringe pump, allows to achieve high percentage of productivity during the time. The advantages of this method comparing to the conventional batch reactions are higher surface-to-volume ratio, easier heat and mass transfer resulting in more efficient and sustainable reaction, and easier control and scale-up.[58] In literature there are many examples of deoxygenation reactions of GL performed in continuous-flow fixed-bed reactors in the presence of zirconium as catalyst (Zr sponge average market price: 26.42 $/kg).[59] It was used as acid-modified for Co-Al catalysts, to increase catalyst acid strength and metal dispersion, leading to a high selectivity for 1,2-PD (85% with 72% of GL conversion) in water and in a vertical fixed-bed reactor at 503 K and 35 bar.[60]

A sequential double hydrogenation reaction in flow was also presented by Luo *et al.*, using modified amorphous zirconium phosphate supported Pt catalysts.[61] The acid sites of the catalysts promoted the selective dehydration of GL into Acr, whereas the Pt sites facilitated H_2 dissociation and sequential hydrogenation of Acr into 1-PO (24% yield). The addition of tungsten to the catalyst improved the results (81% 1-PO yield at 543 K and 20 bar H_2) increasing the acidity of the catalyst and gaining a better dispersion of Pt nanoparticles (Scheme 7).[61]

The reaction conditions (*e.g.*, the operating temperature), and not only the type of catalyst, can also affect the selectivity of GL transformations. Srinivasa Rao's group studied the conversion of GL to Acr using modified zirconium phosphate (ZrP), often used as a water-tolerant and high thermal stable solid acid catalyst.[62] The authors linked the reaction temperature and the catalyst acidity by the varying P/Zr ratio in the GL dehydration in flow: both conversion of GL and selectivity for Acr increased until full conversion of GL and 63% Acr and 2% HAc yield, with increasing P/Zr molar ratio from 0.33 to 2.00 at 590–600 K and atmospheric pressure of N_2. Instead, at lower temperatures, HAc yield increased (up to 19%), due to variations in the activation energies pathways.[62]

GL hydrogenolysis carried out in a vertical fixed-bed stainless steel reactor was also reported with ZrP as support for metallic Ru and CoO.[63] When Ru^0 was added to CoO supported on ZrP, 80% of propanal with the quantitative GL conversion was obtained, in a one-step process, with very satisfactory catalyst stability after 50 h at 543 K and 20 bar H_2. The main product was propanal, instead of Acr, since Co–O species can absorb C=C bond more strongly than ZrP, leading to the Acr hydrogenation while the presence of Ru nanoparticles, able to dissociate the H_2 molecule, promote the catalytic performances of CoO in the GL hydrogenolysis.[63]

The partial substitution in MgAl layered double oxide with Zr enhanced the catalytic activity of this solid compound varying the ratio between acid and basic sites and improving the formation of *in situ* H_2.[64] This modified MgAl was tested in the catalytic hydrogenation of GL at 453 K in 4 h resulting in a higher conversion compared to that observed with MgAl without Zr (37% rather than 13%). Unfortunately, the 1,2-PD selectivity was not high (7%) because of the over-hydrogenation of the diol to ethanol and acetaldehyde, the main final product.[64]

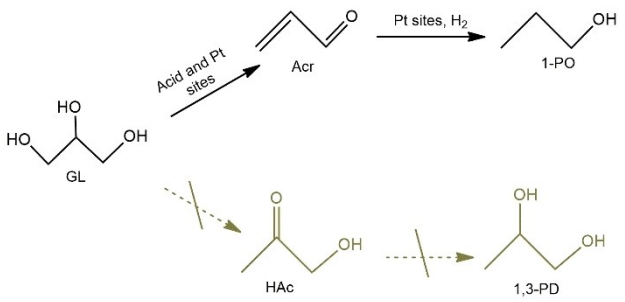

Scheme 7. Reaction mechanism for GL hydrogenolysis to 1-PO with Pt/WO_x-ZrP catalyst. Adapted with permission from R. Luo, X. Zhao, H. Gong, W. Qian, D. Li, M. Chen, K. Cui, J. Wang, Z. Hou, *Energy & Fuels* 2020, 34, 8707–8717. Copyright 2020 American Chemical Society.

2.5. Niobium

Niobium is a TM found in nature not as a pure element but in minerals (Nb average market price: 88.08 $/kg).[65] It shows acidic characteristics so that it is employed as Lewis acid in several different types of reactions (*e.g.*, alkylation, dehydration of polyols, oxidation/dehydrogenation reactions).[66] With five electrons in its outer valence shell, niobium displays rich redox chemistry through oxidation states ranging from −1 to +5.[67] The most common compound of niobium, in nature, is the pentoxide, Nb_2O_5, able to catalyze the oxydehydration reaction of GL into Acr or AAc.[66]

Several are the examples of catalysis involving Nb with W. La Salvia *et al.* synthesized Nb-W-O and V-W-O bronze catalysts onto mesoporous KIT-6 as inert support.[68] The catalyst containing niobium promoted the dehydration of GL to Acr having own acid sites, while the catalyst containing vanadium presented also redox sites, necessary to obtain AAc.

Working in flow at atmospheric pressure, full GL conversion was achieved leading to Acr in 70% yield using Nb-W catalyst at 573 K. On the contrary, V-W-based catalyst promoted the one-pot oxydehydration of GL, catalyzing two different steps: i) the GL dehydration into Acr onto acid sites and ii) the oxidation of Acr into AAc *via* redox sites (V^{4+}/V^{5+}). In this case, the temperature required to speed up the reaction was higher (600 K), also producing an increased amount of carbon oxides and heavy compounds (*e.g.*, GL oligomers and ketals) with about 30% selectivity for AAc. Thanks to the interactions between metal and support, that resulted in a decrease in the number of strong acid sites, the supported Nb-W and V-W catalysts onto KIT-6 showed better Acr and AAc selectivities, respectively. These supported metal oxides minimized the degradation to AAc (with Nb-W) and to other compounds (with V-W) and the selectivity rose from 70% to 78% for Acr and from 19 to 31% for AAc.[68]

In the presence of a series of hydrothermal prepared bronze W-Nb-O catalysts, the selectivity to Acr decreased, favoring the formation of by-products, when the Nb-content in the catalysts increased.[69] A strong presence of Nb promoted a structural change of the oxides (pseudocrystalline phases) increasing the proportion of LAS on the surface, thus promoting the degradation of Acr to heavy compounds.[70]

Niobium was also used to extend the tungstate zirconia catalysts life-stability.[71] The optimal catalytic performance was obtained in presence of $NbWO_x/ZrO_2$ (3% Nb_2O_5) with 81% GL conversion and 72% Acr selectivity, after 24 h reaction at 563 K and atmospheric pressure, in a vertical fixed-bed tubular quartz reactor. The W-Zr catalyst contained both LAS and basic sites. Doping the catalyst with Nb led to an improvement in catalytic activity, probably due to the neutralization of some basic sites on the ZrO_2 support by niobium addition.[71]

Fine tuning the ratio of acid/base sites is fundamental to achieve a good compromise between catalytic behavior and

catalyst's long life. Among the physical-chemical superficial characteristics of a catalyst (many of which could be altered during the calcination step), the presence of acid or basic sites is a property that can be modulated, as seen above. The 8 wt% Nb_2O_5 supported on zirconium doped mesoporous silica (Si/Zr = 5 molar ratio) underwent phosphoric acid treatments varying the Nb/P molar ratio between 0.1 and 1, and modifying acid properties of the catalyst surface.[72] The best results in terms of both selectivity to Acr and catalyst stability were seen when the acid sites had low and moderate strength (Nb/P = 0.2). This synthesized catalyst allowed for achieving a quantitative GL conversion and an Acr yield of 74% after 2 h of time-on-stream, at 623 K, under atmospheric pressure, in a fixed-bed continuous-flow stainless steel reactor. Moreover, the spent catalyst was reactivated by thermal treatment at 823 K without loss of activity.[72]

The impregnation of Nb_2O_5 by Mo/Co or Co/V imperceptibly enhanced the selectivity to Acr (from 74% to 75% and 73%, respectively) but changed the distribution of by-products favoring the formation of the industrially important AAc (10 and 3%) rather than C_2 and C_1 aldehydes, working at 573 K.[73]

The strength and balance between the BAS and LAS are also affected by catalyst preparation method. Stawicka *et al.* synthesized niobium containing SBA-15 by two different methods: one starting from ammonium niobate(V) oxalate and SBA-15 by impregnation method of 15 or 25 wt% of Nb, the other mixing Nb_2O_5 with silica and then calcinating it at 773 K.[74] They found only weak LAS and BAS in the mixing prepared catalyst, while the catalyst obtained by impregnation showed strong BAS, especially for 25% Nb one. Since it is known that the strength of BAS, not its high concentration, promotes the dehydration reaction, to reach a better selectivity of Acr (61 instead 43%), the authors reduced the number of acid sites by silylation, with a considerable decrease in coke formation (from 47% to 27%) carrying out the reaction at 623 K in continuum mode. The reason for this high yield and selectivity of Acr could be ascribed not only to high strength and low concentration of BAS, but also to the proximity of BAS and LAS on the catalyst surface.[74]

Other C_3 products were obtained in the presence of Nb-based catalysts using GL as starting material. Products of reduction can be achieved after Nb doping of other metals so that Nb_2O_5 promotes GL adsorption on catalyst surface and then the interaction of the organic with the metal. 1,2-PD was obtained using Ru/Al_2O_3 (boehmite phase) doped with Nb_2O_5 which played a stabilizing role for Ru nanoparticles avoiding their aggregation.[75] When Nb/Ru molar ratio is about 1 (with Ru 3 wt%), even the smaller Ru nanoparticles (10 nm) were very well dispersed on the Nb-incorporated alumina matrices, allowing the achievement of good results (GL conversion 29% and 1,2-PD selectivity 26%) working in flow continuum mode in H_2/N_2 atmosphere at 531 K and 45 bar.[75]

The Nb addition to a Pd-Zr-Al catalyst favors the reduction of the PdO species and its dispersion on the catalyst surface; at the same time, Nb can enhance the acidity of the catalyst and consequently contribute to increasing the GL conversion in aqueous solution from 37 to 69% and selectivity for 1,2-PD from 78 to 85%, at 473 K and 35 bar H_2; thanks to its high stability, good reusability was observed.[76]

When the doping of 2% Nb was done into a WO structure supporting Pt catalyst, 1,3-PD was the main hydrogenolysis product (30% selectivity with 40% aqueous GL conversion at 433 K, 10 H_2 bar for 12 h of reaction).[77] Employing a simple Pt/WO catalyst, the 1,3-PD yield decreased (from 14 to 8%) increasing H_2 pressure (from 10 to 50 bar) since an over-reduction occurred. However, the addition of Nb to the solid catalyst inhibited the overreduction of W species; in the presence of this Nb-added catalyst, carrying out the reaction at the same temperature and reaction time and increasing H_2 pressure to 50 bar, the 1,3-PD yield was not affected.[77]

Oliveira's research group prepared and tested different catalysts to transform GL to AA. They synthesized a niobium-vanadium-modified silicate and a niobium oxyhydroxide for the simultaneous dehydration/oxidation of GL with hydrogen peroxide at 523 K resulting in a quantitative conversion of the substrate and 14% and 46% AA selectivity, respectively.[47,78]

2.6. Molybdenum

Molybdenum (commonly in the form of sulfides and oxides) is used as a heterogeneous catalyst since it usually can control the rate and selectivity of a wide range of chemical reactions, such as hydrotreating and oxidation. Its average market price is 62.01 $/kg.[79] Molybdenum borides, carbides, nitrides and phosphides are identified as effective catalysts for a range of reactions, *i.e.* hydrodeoxygenation (HDO), hydro-denitrogenation, hydrodesulfurization and syngas conversion.[80]

Recently, the conversion of gaseous GL into AA over Fe-Mo and Cs-Fe-Mo/HZSM-5 (with $SiO_2/Al_2O_3 = 30$ and 1500) catalysts was tested in a packed-bed continuous-flow reactor at 623 K and atmospheric pressure.[81] The reaction showed 52% of AA selectivity at 94% GL conversion with Cs-Fe-Mo/HZSM-5 catalyst. The success of this catalyst was attributed to the presence of basic sites, balanced with acidic sites, to the high mesopore volume (0.072 cm^3/g, only 0.031 cm^3/g in the case of the HZSM-5) and mesopore surface area (103 m^2/g, only 40 m^2/g in the HZSM-5) and to the synergetic interaction between metal species and ZSM-5 zeolite support (in the upper reaction of Scheme 8, the formation of AA was reported; in the other sites all the by-products were displayed).[81]

CeO_2 was also used as support of the bimetal oxides MoFe: the catalyst showed good stability throughout the gaseous conversion of GL to AA, probably due to the small nanoparticle sizes (7–17 nm) and low degree of CeO_2 crystallinity.[82]

HDO reaction can be directed toward different products modifying the surface of molybdenum carbide catalyst to reduce the oxophilicity of Mo by Cu monolayers.[83] Mo_2C was very active in breaking C–O bonds to form propene, but the authors managed to change products distribution depending on the amount of Cu added. Therefore, in the presence of Cu, it was possible to form AA and propanal and, increasing Cu amount, the Cu/Mo_2C surface cleaved only one C–O bond to obtain mainly HAc.[83] Different products were produced by gas

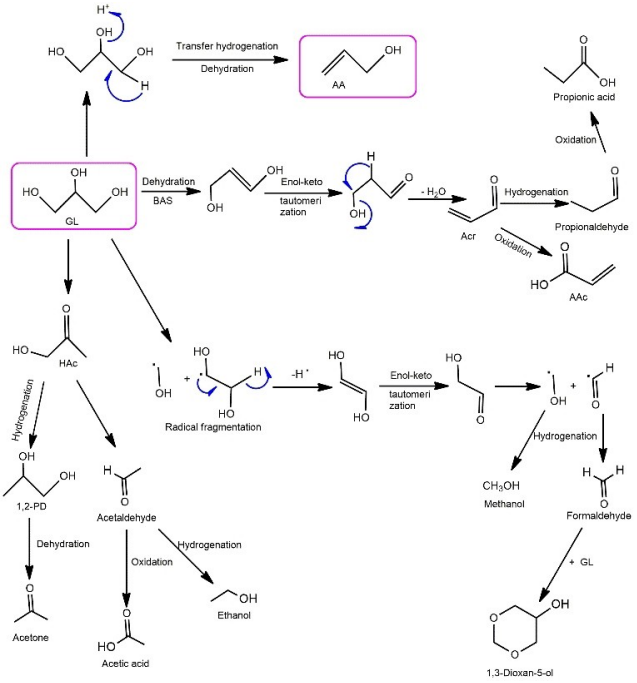

Scheme 8. Full reaction pathway of GL to AA in the presence of the Cs-Fe-Mo/HZSM-5 catalyst by dehydration and transfer hydrogenation. Adapted with permission from A. Kostyniuk, D. Bajec, P. Djinović, B. Likozar, *Chem. Eng. J.* 2020, 397, 125430. Copyright 2020 Elsevier.

phase HDO over a $NiMoS_x/Al_2O_3$ catalyst, depending on reaction time (range between 3 and 360 s) at 673 K and 18 bar H_2 in a packed-bed flow reactor. At short contact times, the main products were unsaturated oxygenates including AA (41% yield), Acr (9%), HAc (21%), and acetaldehyde (4%) while the products detected at longer contact times were alkanes/alkenes (80% yield), CO_x (12%), and saturated alcohols (4%).[84] The authors tried to find a solution to catalyst deactivation by coke, flowing H_2S. With a 2100 ppm H_2S co-feed, the $NiMoS_x$ catalyst showed a 12-time decrease in the deactivation rate for deoxygenation and a 6-time decrease in the deactivation rate for hydrogenation.[84] The production of AA was correlated with the redox sites activity and the surface moderate acid density of catalysts.[85] The catalyst MoFe-0.3/KIT-6, having a good balance between moderate acidity (0.478 $\mu mol\,m^{-2}$) and weak reducibility of catalysts, exhibited a remarkable yield of 27% of AA at 94% conversion of GL without external hydrogen donors.[85]

Mo-based catalysts supported on black or activated carbon catalyzed propene formation *via* one-step GL HDO reaction. Here the use of H_2 was found essential for selective propene production because it converted the intermediate 2-propenol into propene impeding the 2-propenol isomerization to propanal. Moreover, a pre-treatment of the Fe-Mo catalyst at 770 K with H_2 was crucial because it produced the Mo^{4+} and Mo^{5+} active and selective species.[86]

MoO_3 was used as an acidic modifier in a Ni based catalyst (Ni_2P/Al_2O_3), proposing a one-pot two-step synthesis of propene from pure GL in a fixed-bed reactor by hydrogenolysis of GL to propanol and catalytic cracking of propanol to propene with ZSM-5 catalyst, achieving 88% of the desired product at 523 K without H_2.[87] Molybdenum species were used again as modifier: the metal was added on a zirconia-based Pt catalyst to promote liquid-phase GL hydrogenolysis.[88] The different acidity of several modifiers (*e.g.*, W, B, and Mo) were compared, highlighting the correlation between GL conversion and catalyst Lewis acidity at initial 6 bar H_2 and 433 K: $Pt//W/ZrO_2$ was the most active catalyst leading to 42% 1,3-PD with a not so high conversion (around 20%), followed by $Pt//Mo/ZrO_2$ that produced 49% 1,2-PD but with a conversion of only 7%, while $Pt//B/ZrO_2$ was nearly inactive.[88] DFT was used to study the role of α-MoO_3 in the GL conversion to propanal, then its hydrogenation to 2-PO and 1-PO and, finally, dehydration to propene.[89] The authors underlined that this HDO took place on surface vacancy defects of the catalyst by an interaction between Mo species and oxygen of GL: the three-step reaction (dehydration, keto–enol equilibrium and hydrogenation) was found selective to the C–O cleavage instead of C–C one. Exploiting this positive interaction between Mo and GL, the use of 8.7 wt% Mo on black carbon was reported to produce 71% of propene over full GL conversion in vapor phase under continuous-flow conditions at 553 K and 30 H_2 bar; other identified products were the reaction intermediates as propanal, 1-PO and 2-PO, as previously proposed by the DFT.[90]

Bezerra *et al.* promoting the gas phase oxidative dehydration of GL to Acr (at atmospheric pressure and 573 K, in a vertical packed-bed borosilicate reactor) found that its good selectivity was dependent also on the acidity of vanadium and molybdenum oxides supported on Al_2O_3.[42] Unfortunately, the Mo catalyst suffered of higher deactivation by coke deposition.[42]

A study reported several TM hydrogen phosphates supported on meso-HZSM-5 as a hybrid catalyst for the Acr formation *via* GL dehydration. The catalytic activity and selectivity were correlated to the physical (pore characteristics of support) and chemical (moderate strength and appropriate amount of BAS) properties of catalysts.[91] The pore volume of meso-HZSM-5 were 0.28 cm^3/g, larger than that of commercial HZSM-5 (0.15 cm^3/g); in the synthesized meso-HZSM-5, the micropores (< 1 nm) appeared quantitatively diminished and the mesopores (2–4 nm) increased. More strong acid sites are presented in the phosphates supported on meso-HZSM-5; by temperature programmed desorption of ammonia, the strong acid percentage reached 80% in the $Mo_{1/3}HPO_4$/meso-HZSM-5 from 41% of the commercial HZSM-5. The yields of the GL dehydration were found dependent on the employed TM hydrogen phosphates ($CuHPO_4$, $Mo_{1/3}HPO_4$, $ZnHPO_4$, $NiHPO_4$, $MnHPO_4$). The protons provided by hydrogen phosphate acted as a source of strong BAS mediated by the support, which greatly enhanced the yield of Acr. Indeed, the acidic modified TM-HPO_4/meso-HZSM-5 showed high Acr yields ($\geq$70%), with $Mo_{1/3}HPO_4$/meso-HZSM-5 produced 72% of Acr.[91]

Wu *et al.* reviewed in depth many studies about the formation of AAc from GL.[92] Among binary metal oxides (Mo-V-O, W-V-O, Mo-V-W-O, W-V-Nb-O), Mo-V-O catalysts appeared very active to promote one-pot oxydehydration of the GL to AAc in the continuous gas-phase (Scheme 9).[92]

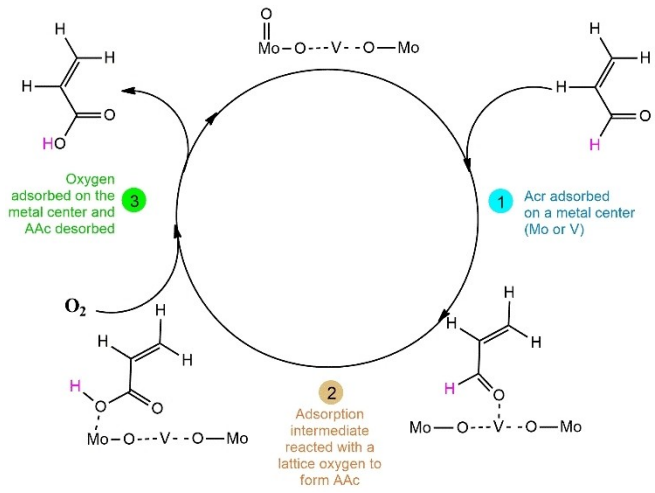

Scheme 9. Oxydehydration of GL to AAc, catalyzed by Mo-V-O catalyst. Adapted with permission from S. T. Wu, Q. M. She, R. Tesser, M. Di Serio, C. H. Zhou, *Catal. Rev. - Sci. Eng.* 2020, 62, 481–523. Copyright 2020 Taylor and Francis Group.

The gaseous atmosphere played an important role in the AAc formation because a raising selectivity and catalyst stability were observed with 100% O_2, due to the equilibrium between V^{4+} and V^{5+} species.[93] The efficiency and the stability of MoVW oxides can also be raised by adding surfactants in the hydrothermal synthesis of the catalysts.[44] MoV_2O_8, among the molybdenum vanadium mixed catalyst, was presented as the most active species for the AAc synthesis at 593 K and atmospheric pressure, since the cycle of reduction and oxidation of the vanadium during the reaction caused pronounced dynamic formation of oxygen vacancies, resulting in 97% conversion of GL and 32% selectivity.[94]

In the oxydehydration of GL, also bifunctional catalyst formed from Keggin-type molybdovanadophosphoric acid, $H_{3+x}PV_xMo_{12-x}O_{40}$ (x = 0–3), and ZSM-5 zeolite was proposed to obtain at 623 K high yields of AAc (35%) and Acr (60%).[95]

2.7. Tantalum

Tantalum is a refractory metal (Ta powder average market price: 324.14 $/kg)[96] used for different purposes in alloys with many other metals.[97] It is oxophilic and frequently present as Ta(V) in the coordination compounds. Due to the oxide film on its surface, tantalum is known to be very corrosion resistant, but it is attacked by HF.[98]

To the best of our knowledge, only in recent works, the use of tantalum in deoxygenated reactions of GL was reported. Pt supported on WO_x-modified tantalum oxide was synthesized as a catalyst for hydrogenolysis of GL to produce 1,3-PD.[99] The crystalline *T*-phase Ta_2O_5 was chosen to act as support for Pt owing to thermal and hydrothermal stability and for its high similarity with W (in electronegativity and ionic radius); in that way, the WO_x dispersion on the support surface can be enhanced.[99]

The WO_x species acted as anchoring sites for Pt without formation of Pt nanoparticles, so an atomically Pt dispersion could be formed on the surface. This peculiarity increased the H_2 absorption capability. The positively charged Pt species in $Pt^{\delta+}/WO_x/T\text{-}Ta_2O_5$ enabled H_2 heterolytic dissociation to $H^{\delta+}$ and $H^{\delta-}$ species, and $H^{\delta+}$ species spilled over the surface of support *via* Pt-O-W interfacial, producing BAS.[99,100] Operating in water solution at 433 K and 50 bar H_2 pressure, a 90% conversion of GL was reached and a selectivity for 1,3-PD of 45%. This catalyst was reused for 4 successive runs, evidencing only a small decrease in GL conversion from 90% to 79%, without changes in the selectivity toward 1,3-PD.[99]

Recently, a mesoporous tantalum phosphate was used in the dehydration of gaseous GL to obtain Acr in a down-flow fixed-bed reactor at room pressure and 573 K under N_2.[101] The catalyst, which exhibited mainly Ta^{5+} species, showed BAS and LAS that favored the formation of the product with >70% selectivity (at 85% conversion).

2.8. Tungsten

Tungsten species (W average market price: 38.19 $/kg)[102] are often employed as co-catalysts in the valorization processes of GL: they can not only enhance the acidity of the catalyst or increase the number of BAS but also improve the dispersion of other active metals. The presence of BAS can promote the hydrogenolysis of GL to 1,3-PD, by absorption of one -OH moiety and subsequent dehydration and hydrogenation steps or by a dehydration to AA, which is easily converted to 3-HPA and hydrogenated.[103]

Garcia-Fernandez *et al.* observed that polytungstates (WO_x) have the appropriate moderate BAS to transform GL to 1,3-PD selectively, establishing structure–activity relationship of these supported bimetallic catalysts (Pt/WO_x on aluminum oxide materials and on a HZSM-5 zeolite), where the proximity of Pt promoted the hydrogenation of the intermediate carbocation into 1,3-PD (56% selectivity with catalyst on alumina).[104] Raising the strength of BAS (HZSM-5 as support), 1,3-PD (21% selectivity) was transformed to 1-PO (35% selectivity) and propane (33% selectivity), while the Pt dispersion made the catalyst more active in terms of reagent conversion (from 8% to 16%) but less selective since even 1,2-PD was produced (1,3-PD/1,2-PD ratio from 3.1 to 2.6).[104] *In situ* growth of hydrate WO_3, on the surface of $\gamma\text{-}Al_2O_3$, encouraged a regular dispersion of Pt species producing their strong interactions with WO_x, and converted 77% of GL to 1,3-PD at 453 K; when this catalyst was synthesized by traditional wet impregnation/calcination, only 39% was transformed.[105] The stabilization of metal single atoms on tungsten oxide and their catalytic properties in H_2 activation were discussed. Pt species on WO_x increased catalyst stability and facilitated the dissociation of H_2 producing BAS ($H^{\delta+}$) under H_2 atmosphere after spillover of hydrogen to WO_x.[106] Shi *et al.* observed the influence of increased acidity and metal dispersity, for the Pt/TiO_2 catalyst when doped with WO_x, on the reagent conversion at the expense of the selectivity: at high conversion, 1-PO was formed with 33%

selectivity, detrimental to the formation of 1,3-PD, obtained with 22% selectivity.[107] It was also pointed out that the polymerization degree of the WO_x domains affected the 1,3-PD yield.[108] WO_x enhanced significantly 1,3-PD formation rate at 453 K and 80 bar, especially after Mn doping of Pt-WO_x/ZrO_2 catalyst, since Mn was able to generate a large amount of medium polymerized WO_x. The authors described Pt-$(WO_x)_n$-H as the catalytically active structure.[108] The high activity of the oligomeric WO_x species was outlined also using a Pt/W/SBA-15.[109]

Wang *et al.* observed that Mg doping on the Pt/WO_x-ZrO_2 catalyst surface inhibited high polymerization degrees of WO_x and, furthermore, the leaching of tungsten, greatly improving catalyst stability.[110] Pt/0.50Mg/WO_x–ZrO_2 catalyst exhibited superior stability with 53% conversion in 25 h time-on-stream at 423 K and 40 bar.[110] Pt/H-WO_3 (with high oxygen vacancies) exhibited higher GL conversion (64%) and 1,3-PD selectivity (43%) than that (38% conversion, 33% selectivity) with Pt/L-WO_3 (low oxygen vacancies), carrying out the reaction at 433 K and 50 bar.[111] This was explained considering that Pt/H-WO_3 can more easily be coordinated by two terminal hydroxyl groups of a GL molecule, while the secondary OH group can be protonated by the $H^{\delta+}$ generated by H_2 on Pt.[111] Liu *et al.* determined that the interface of Pt-WO_x is regarded as the active site for the selective dissociation of C–O bond and, for this reason, the authors' issue was to increase the affinity of Pt and W.[112] It is possible to change the catalyst structure of Pt-WO_x/SiO_2 by modulating the tungsten amount: only the catalyst modified by appropriate small amount of W (W/Pt = 0.25) can work with success at 80 bar of H_2 and 413 K, reaching 83% of GL conversion and 57% of 1,3-PD selectivity.[112] At 413 K and 10 bar H_2, 81% GL conversion and 51% 1,3-PD selectivity were obtained employing Au-promoted Pt/WO_x catalysts, characterized by a high metal dispersion on WO_x.[113]

The use of a bifunctional catalyst (metal/BAS surface) can provide a double effect driving on dehydration and hydrogenation steps together: Ni/WO_3–TiO_2 catalyst afforded 1-PO and 2-PO in total yield of 94% at 513–543 K and H_2 pressure of 20–36 bar.[114] The strong acidity of the catalyst promoted the dehydration while Ni nanoparticles allowed the hydrogenation reaction. Even the H_2 pressure influenced the yield of 1-PO: using 10Ni-30HSiW/α-Al_2O_3 at 40 bar, 85% selectivity was calculated.[115] The H_2 pressure preserved the zero-state of nickel, necessary for the selectivity in the hydrogenation step, while reduced the presence of W^{6+} and, consequently, the acidity of the catalyst and the conversion of GL (55% from 65% at 10 bar).[115]

Trying to shift the dehydration reaction product to Acr using a WO_3/ZrO_2 catalyst in flow mode at 553 K and 5 bar, with H_2 as the gas carrier, Hulteberg *et al.* focused their research on changing the catalyst pore structure, removing pores with diameter <45 Å by thermal sintering at temperatures above 1073 K.[116] In this way, it was possible to obtain a longer life catalyst with a lower specific surface area (11% decreased), more open pore structure (pores larger than 45 Å), a lower absolute acidity but higher specific acid density (from $1.85\cdot10^{-6}$ to $2.05\cdot10^{-6}$ mmol/m^2).[116] In a different study, the results obtained when using WO_3-SiO_2 and WO_3-ZrO_2-SiO_2 catalysts were compared for the gas phase GL dehydration to Acr.[117] The reaction was carried out in a fixed-bed reactor, under aerobic atmospheric pressure and in a temperature range of 553–653 K. The yields of Acr were between 40 and 90%, strongly depending on the catalyst composition (W and/or Zr amount). Usually, the yield decreased when Zr amount increased, maybe due to the formation of other oxidative by-products, *e.g.* CO_x. The authors observed also a parallelism between the selectivity to Acr and the proportion of BAS in catalysts.[117] Dehydration of GL to Acr was achieved using a WO_3/ZrO_2@SiC catalyst, under microwave irradiation, with better results compared to conventional electric heating: at 523 K the Acr selectivity reached over 70% with complete GL conversion under microwave, against 54% by conventional heating.[118] The microwave was used again to prepare, by sol-gel method, a 25%WO_3-SiO_2 that catalyzed the Acr formation (54% selectivity at full conversion) in a fixed-bed reactor at 573 K.[119] The microwave raised the concentration of medium-strength BAS and led to a high amount of cubic WO_3 crystals which increased the catalyst stability.

WO_3/Al_2O_3 catalyst, with 20 wt% WO_3 loading, showed, in the dehydration of GL, higher activity and durability (assessed up to 5 h) than other similar supported WO_3 catalysts and zeolites.[120] By carrying out the reaction at 588 K in a fixed-bed reactor, the number of BAS and mesopores in the catalyst were the same before and after the reaction, extending the catalyst life also under O_2 flow and raising to 90% Acr yield.[120] Recently, tungsten-based heteropolyacids were supported on non-ordered mesoporous silica to catalyze the dehydration to Acr.[121] The Acr formation rate showed a good linear relationship with respect to the BAS concentration and the total acid concentration (Brønsted and Lewis) until $H_3PW_{12}O_{40}$ loading 30 wt%. This relationship changed for higher percentage loading, maybe for a worst dispersion of heteropolyacids that did not allow the linear increase of acid sites number. The authors reported an Acr formation rate in the range of 3.0–5.0 mmol h^{-1} g^{-1} working in a vertical fixed-bed reactor at atmospheric pressure and 573 K.[121]

A hydrothermally synthesis of two different W-V-O catalysts was reported in literature: the hexagonal tungsten bronze (h-WO_3) phase and monoclinic phase (m-WO_3).[122] The h-WO_3 showed a significantly higher concentration of acid sites than m-WO_3, making h-WO_3 active for AAc production (yields of Acr and AAc were 24% and 32%, respectively), while m-WO_3 led to the formation of CO_x. This gas-phase oxydehydration of GL was conducted in a fixed-bed reactor at atmospheric pressure and 593 K.[122]

2.9. Rhenium

Rhenium (Re average market price: 2,395.82 $/kg)[123] is a metal with very specific catalytic performances showing several oxidation states, frequently in very stable forms.[124] For other metals, indeed, it is not common to have stable high oxidation state derivatives at room temperature (*e.g.*, Mn) but Re_2O_7 is

commonly used, in water or oxygenated organic solvents (where it is very soluble), to prepare numerous supported catalysts at 298 K. By taking a brief look at the rhenium chemistry which occurs in any catalytic applications, it is interesting to evidence its peculiarity to activate the C–O bond, then facilitating the bond-cleavage. In this regard, it was demonstrated that the ReO_2^- species, when in its gaseous form, can extract an oxygen atom from CO_2 producing CO and ReO_3^-.[125] As we are considering only reduction reactions, hydrogenolysis and DODH are certainly the two widely diffused reactions where this metal is employed as a catalyst. Hydrogenolysis of GL leads to 1,2-PD or 1,3-PD and Re is often used in association with other TMs. A bimetallic supported Re-Cu/ZnO system was prepared *via* wet impregnation: the presence of Re improved the distribution of metal oxide on the support while the presence of Cu decreased the Brønsted acidity of the catalyst.[126] The supported catalytic system was active for hydrogenolysis of GL in a continuous-flow fixed-bed reactor in a temperature range of 423–523 K and a H_2 pressure of 60 bar. At 423 K, the selectivity to 1,2-PD was excellent (about 100%) but, increasing temperature or H_2 pressure, the formation of minor alcohols, 1-PO (8% selectivity at 523 K) and ethylene glycol (45%) occurred.[126] It is worthy of mention also the work by Varghese *et al.*, which investigated the formation of 1,3-PD when the supported ReO_x-Ir/SiO_2 catalyst was used.[127] Despite we cited the same research in the iridium section, here we highlight the role of Re in the improvement of the 1,3-PD yield (with 1:1 = Re:Ir) to the detriment of 1,2-PD (with Ir only). The reduced Brønsted acidic ReO_x clusters, dispersed on the Ir nanoparticle surface, facilitated dissociative attachment of GL addressing the reaction to a preferential formation of the primary propoxide, with a consequent formation of 1,3-diol. In the presence of a H-ZSM-5-supported similar catalyst, at mild temperatures (393–453 K), the over-hydrogenolysis of diols was inhibited; however, raising pressure from 20 to 80 bar, the conversion and 1,3-PD selectivity were higher (from 8 to 10% and from 14 to 35%, respectively).[128]

As potential DODH products, we can mention AA that can be obtained in good yield employing MTO, Re_2O_7, ReO_3, or other rhenium oxides.[129] A remarkable AA yield (91%) was obtained at 443 K using 10 wt% ReO_x/Al_2O_3, with 2-hexanol as both reductive and solvent agent.[130] The authors confirmed the heterogeneity of the involved catalysis mechanism since the reaction stopped upon removal of the ReO_x/Al_2O_3 by hot filtration and they also evidenced the absence of the metal leaching. The catalyst reuse tests demonstrated its activity for 3 reaction cycles. Mechanistically, the authors proposed a catalysis involving the redox-couple Re^{V}/Re^{VII}. Mesoporous ceria supports, prepared by a nanocasting process with silica as hard template, were impregnated with 10 wt% ReO_x and used in DODH reaction at 448 K using 2-hexanol or 4-methyl-2-pentanol as solvent and hydrogen donor.[131] Quantitative conversion of GL was observed with 88% yield in AA; also this catalyst was recycled 3 times without loss of activity.

Using soluble catalytic systems, the DODH to obtain AA was reported in the presence of several rhenium compounds, among them oxides, phosphine and halide derivatives, in alcoholic solvent or neat conditions.[129] Lupacchini *et al.* found that, independently of the starting Re species (*e.g.*, oxides, iodides, phosphine), based on IR and XPS measurements, the formation of a Re-alkoxide precipitate was observed and was proposed to be the active catalytic species for all the used Re-catalysts, in alcoholic solvents or in neat conditions; in these last tests GL acted, simultaneously, as reactant, solvent and reducing agent.[129] The reactions in solvent were conducted in 2,4-dimethyl-3-pentanol at 413 K, under air or H_2 flux. The best yields of AA were observed in solution with ReO_3 (91%) and MTO (86%) and under hydrogen gas flux. $Cp^{tt}ReO_3$ (Cp^{tt} = 1,3-di-tert-butylcyclopentadienyl) was reported as the catalyst in 3-octanol under N_2 atmosphere at 408 K able to convert quantitatively and selectively the GL to AA.[132] In this work, the real catalyst species was not identified but the authors observed, during the reaction, the dissociation of the Cp ligands. An improvement in DODH was obtained using ionic liquids as reaction media.[133] When benzyl or imidazolyl derivative was used, good yields of alkene derivatives were observed, and it was possible to reuse the rhenium catalyst, seeing only a slight decrease in product yield. The preserved activity of the rhenium catalyst is probably due to the involvement of the ionic liquid with the resulting suppression of the polymerization of by-products (*e.g.*, HAc, lactic acid, and glyceraldehyde, recovered for the first time at the end of DODH reaction).[133]

3. Late Transition Metals

3.1. Iron

Iron has been considered an attractive metal, mainly due to the redox cycle Fe^{3+}/Fe^{2+}, but also because it is an element easily available, at low cost (pig iron average market price: 0.471 $/kg)[134] and less toxic than vanadium, tungsten or molybdenum.[135] Many articles in literature reported the use of phosphates as catalyst for the hydrogenation of GL since they showed better catalytic behavior than other supports such as zeolites, and they suffer less deactivation. This was confirmed during the gas phase GL dehydration on mesoporous $AlPO_4$ and modified $AlPO_4$ with a small amount (1 wt%) of a TM (Co, V, Fe), calcined at 623 K and 723 K.[136] The best GL conversion (around 90%) was obtained for the Fe catalysts, followed by those with Co (75%) and V (50%), performing the reaction in a continuous-flow fixed-bed microreactor at 553 K under atmospheric pressure. The main product obtained with Fe catalysts was Acr (44% selectivity with $FePO_4$).[136] The crystallinity and the acidity of the iron phosphates were crucial: a quantitative conversion of GL with 82% Acr selectivity was observed only in the presence of the amorphous Fe catalyst.[137]

Despite their easy deactivation, several examples of zeolites, used as support for iron, were reported. Diallo *et al.* prepared catalysts for the GL transformation to Acr with different iron contents and different Si/Al ratio.[138] The role of Fe was just to reduce the catalyst deactivation by altering the amount and the nature of the coke components. In this way, and with high Si/Al

ratio, the Acr selectivity was about 80% performing the reaction at 593 K under atmospheric pressure.[138] H,Fe-MCM-22 was studied as catalyst for gas-phase oxydehydration of GL to AAc and Fe^{3+} oligomers and iron oxide clusters were identified as the main iron species contained in the catalyst structure.[135] The authors observed an inverse relationship between the content of iron with the acid sites density and the textural properties: the catalysts containing the lowest iron amount (1.2%) had shown better yields to AAc (25% instead of 13% with Fe 4.5 wt%). To obtain a higher GL conversion, a balance between acid and textural properties was tuned: 93% GL conversion with 57% AAc selectivity was obtained using 1.2 wt% of Fe in the catalyst and working in a fixed-bed vertical reactor under oxygen feed, using both to warrant the regeneration of Fe^{3+} and to avoid the formation of carbonaceous deposits on the catalytic surface. The evidence that Fe^{3+} tetrahedral species, contained in catalytic framework, were more selective to AAc, while $Fe^{2+}O_x$ clusters in extra-framework position increased Acr selectivity was indicated.[139] The authors synthesized Fe-containing zeolites through two different processes, based on hydrothermal synthesis or post-synthesis preparation. The catalyst obtained by post-synthesis method, with Si/Al molar ratio = 45, showed the reduction of crystallite size and the enhancement of the external surface, leading to 99% GL conversion and 96% selectivity to Acr (no AAc amount), after 30 h on-stream at 593 K and atmospheric pressure. The catalyst obtained by hydrothermal process showed almost the same activity but different selectivity (Acr 71%, AAc 24%) thanks to the Fe^{3+} tetrahedral species in the framework catalyst.[139]

Martín *et al.* presented Fe, Ni and FeNi oxides supported on commercial mesoporous alumina as catalysts in the dehydration-dehydrogenation reaction of gas phase GL at 573 K and ambient pressure.[140] The authors observed that, in these bimetallic catalysts, the presence of nickel reduced the iron oxidation state, enhancing the redox properties of the solid. Moreover, the combination of the two metals changed the selectivity towards the AA (90% GL conversion and 90% AA selectivity) whereas with the monometallic oxides, 88% HAc selectivity was reported.[140] The addition of potassium species to α-Fe_2O_3 yielded a loss of LAS and, in the presence of formic acid, morphology changes of solid were observed with the formation of BAS.[141] Using these catalysts in the dehydration of GL at 623 K, AA was obtained as the main product (40% yield, Acr 10%, others 25%).

The use of iron in combination with other TMs was also described: the electron interaction between Pt and Fe was the cause of enhancement of 1,2-PD yield from GL hydrogenolysis.[142] Pt/Al_2O_3 and Pt/Fe_2O_3-Al_2O_3 catalysts having different Fe/Pt ratios were compared: thus, by increasing Fe loading, it was possible to go from 16% GL conversion and 14% 1,2-PD selectivity (without iron) to 94% GL conversion and 51% 1,2-PD selectivity (Al/Fe = 1/1 atomic ratio), under N_2 pressure at 523 K.[142] The same trend was underlined by Zhang *et al.*: the Fe(OH)O species in Pt-Fe^{3+} enhanced BAS and the faded Pt-H binding strength, thus resulting in 3-fold enhanced selectivity toward ethylene glycol and 1,2-PD (combined selectivity of around 70% when the conversion of GL up to 60%), compared to monometallic Pt supported on zeolite catalysts.[143] A synergistic effect between Fe and Co was also found: Co was able to improve the activation of hydrogen, and Fe improved the acidity of Co-Fe alloy resulting in the formation of AA, from dehydration - hydrogenation, and 1-PO, *via* consecutive hydrogenation of AA, in case of higher reaction temperature and hydrogen pressure.[144]

3.2. Cobalt

Despite its sensitivity to the temperature (Co powder average market price: 29.595 $/kg),[145] cobalt was also used for deoxygenation of GL, being a very active catalyst hydrogenation.

Cobalt oxide (10 and 20 wt% Co) supported on synthetic mesoporous aluminum phosphate and Al-Co phosphates (10 wt%–37 wt% Co) were prepared and used in oxydehydration of gaseous GL to AAc, *via* Acr, at 553 K in a continuous-flow fixed-bed reactor in presence of O_2.[146] Comparing the Co catalysts with the corresponding Fe and V ones, the Co-based were the best catalysts, able to produce AAc thanks to the balance between redox and acid properties.[146] Mesoporous $AlPO_4$ was modified with a lower percentage of Co (1 wt%), and compared it to that with other TMs (Cu, Cr, Fe): Co catalyst showed the maximum yield to Acr (54% with almost quantitative conversion of GL) at 553 K, using a continuous-flow fixed-bed microreactor.[147] The performance was better for Co on $AlPO_4$ comparing to Co supported on some commercial zeolites, like H-ZSM-5 or H-Y.[147]

Two examples reported the use of Cu-Co catalysts supported on alumina for the continuous hydrogenolysis of GL to 1,2-PD.[148,149] Raju *et al.* tested the reaction at atmospheric pressure by moving the temperature in the range of 453–513 K.[148] Co doping induced a fast reduction of CuO species, and the active interactions Cu-Co led to high Cu dispersion (from 35% without Co to 50% in 10%Cu-7%Co) and metal surface area (from 234 m^2g^{-1} without Co to 338 m^2g^{-1} in 10% Cu-7%Co). The catalyst with 10%Cu-7%Co on Al_2O_3 converted completely GL with 77% selectivity to 1,2-PD and it turned out to be very stable.[148] Different Co-Cu/Al_2O_3 with a fixed Cu loading of 7 wt% but a variable Co loading from 0 to 1.5 wt% were prepared, to evaluate the effect of Co.[149] The presence of Co increased the hydrogenation rate of GL up to the plateau due to the raising number of acid sites and to the geometry of the metal species but, above 1.3 wt% of Co, a decreasing of catalytic activity was observed, owing to the formation of aluminates and less acidic sites. However, at 493 K and 5 bar of H_2, the main product was always 1,2-PD.[149] Also in the absence of Cu, a Co/Al_2O_3 was employed in water solution but the conversion and 1,2-PD selectivity were 54% and 76% carrying out the reaction in a fixed-bed flow reactor at 503 K and 35 bar.[150]

The presence of Co^0 nanoparticles is very important: a hydrotalcite-derived Co_2-Ca_4-Al_3 catalyzed several steps for the formation of 1,2-PD.[151] XRD characterization revealed the formation of a $CaCO_3$ layer on the surface of the catalyst that reduced the number of strong basic sites, enhanced the

number of moderate basic sites, and helped to avoid the metals leaching during the reaction, carried out at 483 K and 40 bar H_2 in a continuous-flow fixed-bed reactor. So, the product was obtained with excellent selectivity (91%) at complete GL conversion.[151]

Cobalt aluminate nanoparticles were also used as catalyst in the gas phase GL transformation. They were prepared by flame spray pyrolysis and employed for the catalytic reaction at 573 K and 1 bar H_2.[152] After 3 h reaction, 35% of GL conversion to a mixture of HAc (19%), PAl (23%), lactic acid (8%) and lactide (27%) as main products, was observed.[152]

3.3. Nickel

Although nickel is not a noble metal (Ni briquettes average market price: 18.268 $/kg),[153] nevertheless it can catalyze the hydrogenolysis of GL in a good way. Recently, a monometallic Ni catalyst, supported on CeO_2, was used at 20 bar and 503 K to obtain 1,3-PD.[154] The same catalyst was prepared by two methods: wet impregnation and by ultrasound, the last one being the most successful because of its homogenous distribution, smaller crystallite size, bigger surface area and low reduction temperature. In the presence of the sonochemically synthesized catalyst, 54% GL conversion, 1,3-PD (53% selectivity), 1,2-PD (15%), 1-PO (19%) were obtained.[154]

A series of bimetallic oxides (Ni, Cu or Zn with Zr) was tested supporting them on H-beta zeolite with loading of 5–20 wt% *via* wet impregnation.[155] The most active catalyst in the GL hydrogenolysis was Ni-Zr that gave 1,3-PD selectivity of 14% over 73% GL conversion at 473 K and 41 H_2 bar.[155] In order to modify the acidic characteristic of a catalyst employed in the production of glycols, ion exchange was a viable pathway. Decreasing acidity of the bifunctional catalyst 10Ni-30H_4SiW/Al_2O_3 was reported by the exchange of H^+ with Cs^+, without altering the Keggin structure.[156] The catalysts with Cs ions almost did not influence the GL conversion but affected the products distribution. The authors, working at 513 K and 60 bar H_2, observed that with 10Ni-30Cs1$H_3SiW_{12}O_{40}/Al_2O_3$ it was possible to reach the best selectivity for 1,3-PD and 1-PO and that, in the absence of Ni, the catalyst activity was poor. However, 10Ni-30$Cs_4SiW_{12}O_{40}$, with all the protons substituted by Cs^+, had low selectivity for 1-PO and high selectivity for 1,2-PD and ethylene glycol.[156]

Although even the Cu/Al_2O_3 was an effective catalyst in the hydrogenolysis of GL to 1,2-PD at 523 K and 40 bar H_2 (full conversion and 70% yield), it is interesting to spare the hydrogen gas, obtaining the same very good results.[157] Freitas *et al.* obtained 25% yield of 1,2-PD, at the same conditions, but under an inert atmosphere, using $CuNi/Al_2O_3$ or CuNi/ZSM-5, prepared by wet impregnation and containing 20 wt% of CuO and NiO.[157] The formation of a physical alloy of the two metals was detected by XRD: Ni had the role of promoting the formation of H_2 *in situ*, consumed to hydrogenate HAc, the intermediate obtained during the first-step of dehydrogenation, leading to the desired 1,2-PD in the second one-pot step (about 25% of yield with both supports).[157] Yield and conversion were improved when a copious amount of NaOH (NaOH/GL = 0.5 molar ratio) was added to the reaction mixture containing CuNi/Y as catalyst: the GL conversion raised from 17 (0 mol NaOH) to 97% and the 1,2-PD yield from 3 to 32% in a fixed-bed at 533 K in absence of H_2.[158] The preparation of 1,2-PD was also investigated using 20 wt% Cu–Ni (1 : 1)/γ-Al_2O_3 bimetallic catalyst, charged in a packed-bed down-flow tubular reactor.[159] Full GL conversion and excellent 1,2-PD selectivity (90%) at 493 K and 7.5 bar were observed when the catalyst was previously calcined at 673 K. Calcination temperature was the key factor to the formation of bimetallic Cu-Ni and metal-support phases leading to high metal dispersion (about 20%) and surface area (30 $m^2 g^{-1}$), and small average crystallite size ($\leq$ 20 nm). The authors concluded that, at 673 K, total acidic strength was maximum, diminishing with higher temperature because of metal particles sintering.[159] The dispersion of metal particles onto the solid support and the formation of the suitable acid sites can be gained also with the addition of Ag, like in Ni-Ag/γ-Al_2O_3, active and selective towards 1,2-PD formation.[160]

A comparison between alumina and silica, used as support for Re-promoted nickel catalysts, synthesized by wet impregnation and used in the transformation of GL to 1,2-PD, was published.[161] The reactions were performed in a continuous-flow fixed-bed reactor in a temperature range of 523–598 K and at H_2 pressure of 60 bar. The alumina catalyst was found to be more active than the silica at any temperature in the range but with the formation of mono-alcohols at higher temperature or pressure. The results of this Re-promoted nickel catalyst on the alumina were ascribed to higher metallic surface areas and BAS number.[161] Moreover, the addition of Pt to Ni catalysts seems to be helpful: a Pt-Ni/γ-Al_2O_3 catalyzed the hydrogenolysis to 1,2-PD (52% selectivity and 71% conversion) at 513 K under 10 bar of inert gas.[162]

A Ni-WO_3, supported on modified-sepiolite, was successful in the hydrogenolysis of GL (88% conversion) at 453 K and 20 bar H_2 in the presence of NaOH, producing 1,2-PD with 97% selectivity.[163]

To improve the activity of Ni catalysts supported on a silica-carbon composite in the formation of 1,2-PD, Gatti *et al.* used two alternative strategies.[164] The first strategy consisted in a modification of the catalyst acidity functionalizing the carbon support by oxidation at 353 K with HNO_3 to increase the number of LAS. The second strategy relies on a modification of the metallic phase, producing a NiZn alloy by the addition of small quantities of Zn (1–1.8%). In this last case, 1,2-PD was obtained with 87% of selectivity and 59% GL conversion at 533 K and 20 bar H_2 pressure (85% selectivity and 52% conversion with modified support catalyst).[164] A MgO/Ni_3C catalyst, also in absence of H_2 and of solvent, was usefully employed to transform 74% GL to 1,2-PD (67% selectivity) and HAc (13%) at 513 K.[165] The catalyst was recovered, washed and calcined to reuse it with sufficient activity for 6 cycles diminishing the conversion of 20%.[165]

Ni-based catalyst supported on TiO_2 was also investigated: $Ni/Cu/TiO_2$ catalyst efficiently catalyzed the hydrogenolysis of GL to 1,2-PD, under N_2 atmosphere (35 bar) and using 2-PO as

the hydrogen source.[166] Compared to the same catalyst supported over alumina (Ni/Cu/Al_2O_3), the use of titania as support gave a better selectivity to 1,2-PD (74% *vs* 66% without H_2, 87% *vs* 83% with 35 H_2 bar) and conversion (85% *vs* 78% without H_2, both 100% with 35 H_2 bar) at 500 K, due to the high Cu dispersion (10.4% *vs.* 5.1%) and the right Ni/Cu atomic ratio (1.30 *vs.* 1.13) on catalytic surface. Unfortunately, metal particles sintering and absorption of organic species on the surface led to a rapid deactivation of the catalyst.[166] Mixed oxide of Cu-Cr doped with NiO on γ-Al_2O_3 was tested for gas phase GL hydrogenolysis at 473 K and 3–5 bar in a flow system reactor to produce 1,2-PD and HAc, as by-product.[167] In this case, the glycol selectivity was directly related to temperature and pressure increasing up to 95% with 85% GL conversion (at 5 bar and 493 K).[167]

Nanometric Ni phosphides, in presence of citric acid, demonstrated to act as a chelating agent, proved to be a good catalyst to produce 1,2-PD under N_2.[168] After the calcination step, the residual amounts of citric acid assisted the dispersion of metal particles avoiding the sintering, and supported the initial reduction of the Ni species.

1-PO was obtained in a two-step reaction, using two Ni-based catalysts: first, Ni/γ-Al_2O_3, and then, nickel on carbon-based support modified with phosphorus.[169] It was noted that the excellent selectivity (71% at 533 K and 65 bar) was due to the surface acidity of the second catalyst, correlated with the amount of phosphate species content.[169] The same research group prepared also Ni phosphide on mesoporous carbon to catalyze the transformation of aqueous GL, allowing 74% of 1-PO selectivity with full conversion at 533 K and 20 bar H_2.[170] They noted a different activity for several contents of the phosphate precursor, $Al(H_2PO_4)_3$: when it was between 4 and 10 wt%, the catalyst was more acidic and it was turned out more active, while with a higher content, the catalyst activity increased but the selectivity decreased, due to the strong contribution of dehydration reactions on the support acid sites.[170]

A bimetallic catalytic system, such as Ni/WO_3 supported on TiO_2 or ZrO_2, was prepared by co-precipitation of WO_3-ZrO_2 or WO_3-TiO_2, and catalyzed the GL conversion to 1-PO and 2-PO in a flow system.[171] Working at 523 K and hydrogen pressure of 30 bar, the total yield of propanols was 94% over full GL conversion, with strong prevalence of 1-PO (80% with catalyst supported on zirconia and 88% with catalyst supported on titania).[171] The high dehydrating activity needed to transform GL to carbonylic compounds in the first steps of the reaction was secured by the presence of BAS in the catalyst structure, while the presence of Ni nanoparticles enhanced the extent of hydrogenation to propanols (Scheme 10).[171]

Nickel-substituted tungstophosphoric acid on Y-ASA (porous amorphous silica-alumina) was used as catalyst in the GL dehydration.[172] The presence of nickel enhanced the BAS and LAS of the catalyst and, consequently, its selectivity for the Acr production gaining 74% at 593 K and atmospheric pressure in a fixed-bed stainless steel reactor.[172]

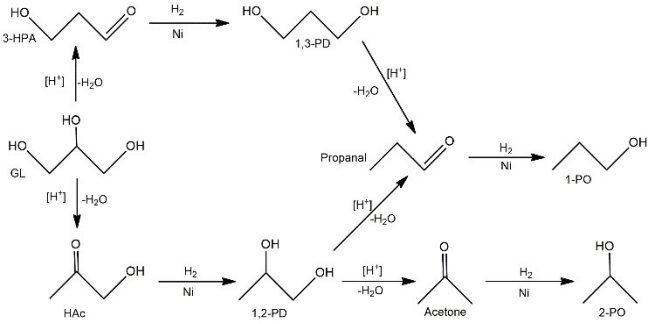

Scheme 10. Mechanism of GL hydrogenolysis to propanols on a bifunctional catalyst (Ni/WO_3 supported on TiO_2 or ZrO_2). Adapted from A. A. Greish, E. D. Finashina, O. P. Tkachenko, L. M. Kustov, *Molecules* 2021, 26, 1–16.

3.4. Copper

Copper is one of the most utilized TM catalysts in synthetic organic chemistry, thanks to its economic (and environmental) advantages arising from its high Earth abundance, compared to precious TM catalysts (Cu average market price: 8.357 $/kg).[173] Also in this review, copper is cited in a lot of papers since it has been employed alone or, often, in combination with other metals, reaching excellent results.

Copper chromite and Cu/Al_2O_3 catalysts had very different physical and chemical properties; however, in the hydrogenolysis of GL, carried out in a trickle-bed reactor, 97% selectivity of 1,2-PD and complete conversion of GL were obtained for both catalysts at 503 K and 14 bar H_2.[174] This comparable activity would be related to the presence of Cu^0 species in both catalysts, as seen by XPS. The authors observed also that higher temperatures produced a decrease in the selectivity to 1,2-PD due to the formation of different by-products: minor alcohols in presence of Cu/Al_2O_3, and HAc and 3-HPA in the case of copper chromite.[174] In the range 473–493 K, a catalyst consisting of Cu-Cr oxides with NiO supported on γ-Al_2O_3 led to an increased selectivity for 1,2-PD, in spite of HAc.[167] The reactivity of copper chromite catalyst in the hydrogenolysis of GL was also studied by DFT showing that the interactions with the substrate were due to both Cr-O and hydrogen bonds.[55] In particular, after the adsorption of the substrate on Cr, the C–O cleavage was favored and the Cu atom promoted the dehydration step to HAc, being the rate-determining step of GL hydrogenolysis.[55]

Lower conversion (72%) and 1,2-PD selectivity (86%) were achieved with the catalyst Cu-Ni/Al_2O_3 at 483 K and 45 H_2 bar with a pseudo-first-order kinetics with respect to GL concentration.[175] Moreover, the kinetic study showed that dehydration of GL to HAc took place on the acidic centers of the catalyst whereas the hydrogenation of HAc to 1,2-PD took place on the metallic sides.[175]

The performance of Cu/Al_2O_3, compared with individual copper particles, was studied in liquid-phase hydrogenolysis, obtaining a linear relation of the reaction rate with specific surface area of copper.[176] Both catalysts, at 473 K and under pressure of 20 bar, gave 98% 1,2-PD selectivity, but the presence of support was able to prevent intensive sintering of

the active phase of the catalysts.[176] The addition of a co-metal such as Ba, Ce or La on γ-Al_2O_3 was a very efficient method to avoid any sintering event, stabilizing the Cu particle size during reaction, consequently increasing the lifetime of the catalyst to 70 h, while the bare Cu catalyst exhibited marked deactivation after only 50–60 h reaction.[177] Furthermore, carrying out the reaction at 473 K and 75 bar in a fixed-bed reactor, the selectivity to 1,2-PD grew up to 96% if the co-metal was Ba, even if the conversion was modest (18%).[177] The geometry of active phase in Cu/Al_2O_3 was indicated as not crucial as its chemical composition.[178] This statement was deduced from the observed higher activity of the Cu_2O phase in comparison with the CuO phase of the catalyst and from the almost same results for catalysts characterized by different particle sizes (20–140 nm) but close chemical composition, with a 98% selectivity for 1,2-PD, at 473 K.[178]

Vila *et al.* performed DRIFT and ^{1}H NMR spectra revealing that the enediol species (1,2- and 2,3-enediol), formed in the hydrogenation reaction of GL, were mainly stabilized at the surface of the reduced Cu/γ-Al_2O_3 catalyst (Scheme 11).[179] Therefore, an increase of surface metallic copper in the catalyst should be a focus to improve the 1,2-PD selectivity by the stabilization of 2,3-enediol. Cu-based oxide, derived from hydrotalcite-like structured catalyst, that exhibited a metallic surface area of 21 m^2/g, catalyzed the formation of 1,2-PD (84% selectivity and conversion) at 40 H_2 bar and 483 K; the same catalyst, but with a metallic surface area of 12 m^2/g, transformed only 57% of aqueous GL (1,2-PD selectivity, 69%).[180]

Starting from Cu and Zn hydroxides as precursors, a copper carbide (Cu_xC) composite, with Cu/Zn = 8, was obtained by thermal treatment/hydrogen reduction.[181] In flow, GL was quantitatively converted and 92% 1,2-PD selectivity at 513 K and 20 H_2 bar was observed. This activity, 10 times over than that of metal Cu in the same conditions, was due to its dispersion in the presence of ZnO and to the acidity provided from Zn species.[181] The fine dispersion of copper oxide particles

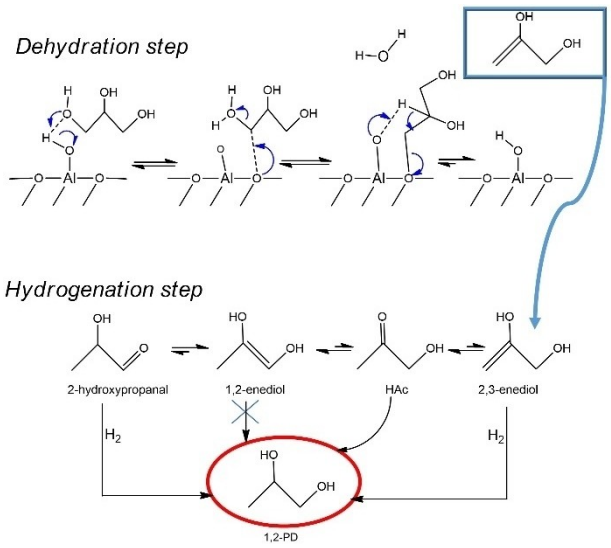

Scheme 11. Mechanism of GL hydrogenolysis to 1,2-PD over Cu/γ-Al_2O_3.

onto $Mg_9Al_{2.7}$-$Ga_{2.3}O_2$ helped the catalytic activity giving a full conversion of gaseous GL to 1,2-PD at 493 K and 5 bar.[182]

The monometallic Cu catalyst supported on γ-Al_2O_3 or on TiO_2 was tested at 553 K under N_2 atmosphere for the production of HAc, resulting more active than the bimetallic system (*i.e.*, Cu-Ni) supported on the same solids.[25] The best results between copper (5 wt%) on γ-Al_2O_3, ZrO_2, or SiO_2 were obtained when ZrO_2 was the support, due to the highest quantity of acidic sites, with metallic copper more homogeneously distributed and dispersed at the catalyst surface.[183] The use of SiO_2 in these cases was never advantageous due to its insufficient acidity. However, Mazarío *et al.* modified the acidity changing the size of CuO nanoparticles: so, CuO appeared more dispersed on SiO_2 increasing their activity and their acid sites density.[184] This catalyst fully converted GL to HAc (selectivity >80%) using CuO of 2.9 nm on commercial fumed silica in a tubular fixed-bed reactor at 533 K.[184] Cu(10 wt%)/SBA-15 catalyst was prepared by simple grinding and used for liquid-phase GL hydrogenolysis at 503 K and 40 H_2 bar affording 97% selectivity of 1,2-PD (on 90% of conversion) thanks to Cu-O-Si-O interface structures (not highly present on the catalyst prepared by impregnation).[185] These interface structures were the origin of the LAS, useful to dehydrate GL to HAc, the potential intermediate in hydrogenolysis, that was hydrogenated onto the close Cu^0 sites.[185] The search for greening these hydrogenolysis reactions led to use ethanol as an *in situ* hydrogen donor; in the presence of a Cu-Al-Zn catalyst, synthesized by co-precipitation, 1,2-PD was produced at 473 K and 30 N_2 bar with 69% selectivity.[186]

MgO was also used as support for copper by preparing Cu and Cu-Ru catalyst on MgO with different amounts of Cu and Ru but with a total metal loading of 10 wt%.[187] The best results (98% conversion, 97% 1,2-PD selectivity) were obtained with 6Cu–4Ru/MgO catalyst in a flow reactor at 493 K and 8 bar, while at atmospheric pressure, the main product was HAc (80% yield; 1,2-PD 15% yield). The catalytic activity was attributed to a good synergy between the copper and ruthenium that was a *reservoir* of hydrogen to spillover it to the Cu.[187] Not-hazardous Cu-based mixed oxides derived from hydrotalcites were also used as catalysts in a continuous-flow fixed-bed reactor.[188] Cu-Mg-AlO_x led to 60% HAc selectivity with almost full GL conversion at 513 K and under atmospheric pressure. FT-IR and XPS measurements evidenced that the presence of Cu, especially the most active Cu^+ species, was essential to carry out the dehydration with high reaction rates.[188] A series of copper-based catalysts supported over magnesium oxide or hydroxide fluoride were tested in gas phase at 573 K and atmospheric pressure.[189] The best catalyst (Cu-MgF_2) led to 82% conversion and HAc in 45% yield, due to an adequate number of LAS and the ability to stabilize the Cu^+ species, while the catalytic activity was very low for Cu-MgF(OH) and Cu-MgO.[189]

Montmorillonite is an active support that shows BAS and LAS and it can support several metallic species; in particular, Cu_2O/montmorillonite, prepared by hydrothermal method, catalyzed the oxydehydration and hydrogenolysis of GL, using H_2O_2 and dimethylformamide as solvent, at 353 K and room

pressure.[190] The authors obtained 72% selectivity to AAc and 10% 1,2-PD with full GL conversion. They proposed a mechanism involving dehydration of GL to HAc on the acid sites of montmorillonite forming 1,2-PD, which was converted to AAc by dehydration on acid sites and oxidation steps by Cu_2O.[190]

The search for high specific surface area supports with particular morphologies is a trend study to understand and improve catalytic performances. Spherical hybrid ZnO/PAAH mesospheres (PAAH = polyacrylic acid) were developed from the 3D self-assembly of ZnO nanoparticles.[191] In order to keep a high specific surface area, the synthesis of Cu supported on ZnO/PAAH was carried out.[191] The ethanol washing and calcination steps contributed to an increase in the specific surface area by decreasing Van der Waals interactions between particles. This characteristic was the reason for the no-sintering copper process, during the reaction, even when a high Cu loading (35%wt) was used. The catalyst showed 70% conversion and 90% selectivity for 1,2-PD performing GL transformation at 473 K and 30 H_2 bar.[191] The authors prepared also Cu/ZnO/$ZnAl_2O_4$/PAAH by sol-gel method where Cu nanoparticles had 4–13 nm size, obtaining full conversion with selectivity 80–90%.[192]

An interfacial bimetallic (Pt and Cu) synergetic effect at the atomic scale, boosted by the SAA (single atom alloy) approach, was reported.[193] PtCu-SAA catalyst was prepared from a hydrotalcite precursor leading to quantitative GL conversion and full selectivity for 1,2-PD at 473 K and 20 H_2 bar. The TOF value was 8–120-fold larger than that of metal catalysts ever reported in the same reaction conditions. Theoretical calculations identified the active sites being at the interface of PtCu–SAA, where a single Pt atom enabled the cleavage of C–H bond on the central carbon and a close Cu atom was responsible for terminal C–O bond breaking.[193]

Ardila *et al.* reported the preparation and the use of bimetallic Cu-Pd/TiO_2-Na catalyst in the HDO reaction.[194] They obtained 93% 1,2-PD selectivity at 60% of substrate conversion, working in aqueous phase at 493 K and 7 bar H_2. The excellent selectivity was imputed to the formation of CuPd alloy nanoparticles in the catalyst. The presence of the alloy avoided the leaching of Cu particles stabilizing the solid; furthermore, Pd species promoted the generation and the activation *in situ* of hydrogen from GL reforming.[195]

Lately, copper Keggin-like catalysts were used to produce propanols: Cu with tungstosilicic acid, supported on γ-Al_2O_3, in continuous-flow fixed-bed reactor at 613 K and 50 H_2 bar, converted 98% GL with 78% total selectivity (71% 1-PO, 7% 2-PO).[196] However, the formation and deposition of condensation products, mostly polyaromatic, deactivated this catalyst that could be protected varying its synthesis procedure with a major amount of tungstosilic acid.[196]

3.5. Zinc

Zinc is not a very expensive metal: its average market price is 3.261 $/kg.[197] Many examples of copper–zinc catalysts in hydrogenolysis reaction of GL were reported.[198] Pandey *et al.* modulated the acidity and basicity of the catalyst, inserting (basic or acid) doping metal oxides in the catalytic composition, to disclose their correlation with the successful of catalytic performances.[199] Among all studied catalysts, Cu-Zn/MgO was the most selective for vapor-phase hydrogenolysis to 1,2-PD: it provided 98% conversion of GL with 89% selectivity at 493 K and 7 bar H_2 thanks to its basicity, its active metal surface and its high metal dispersion.[199] Biswas's research group identified, other than in the appropriate basic character of Cu-Zn/MgO, also in the high amount of hydrogen spillover on the surface and in the easy reduction of CuO in the presence of Zn species, the excellent activity of these catalysts.[200,201]

A fixed-bed reactor with a ceramic membrane (Figure 3) led to the formation of microbubbles-in-liquid over the solid Cu-ZnO at 473 K, affecting the mixture system and the good selectivity for the 1,2-PD (> 92%).[202] The classic Cu/ZnO was prepared from Cu_3(benzene-1,3,5-tricarboxylic acid)$_2 \cdot 9.4(H_2O)$,through calcination and reduction steps, and it was constituted by ZnO nanoparticles dotted on Cu hybrid ($Cu_{1.1}$/ZnO).[203] This catalyst was tested at 523 K in a fixed-bed reactor: the GL was fully converted to 1,2-PD with selectivity over 80%.

Cu/ZnO based catalysts are promising catalysts, but they suffer of deactivation during hydrogenation. The reason seemed to be the zinc species leaching by acid attack, followed by the copper sintering.[204] Moreover, the presence and the amount of initial water in the reaction mixture influenced the final yield and the lifetime of the catalyst.[205]

In some cases, Zn support was doped with Al, to increase its acidity and adsorption capacity for metals. Chimentão *et al.* compared Cu and Ni supported on ZnO with or without Al.[206] The addition of Al promoted the GL conversion: after 4 h of reaction, a conversion of 100% was observed with Ni/ZnAl (with Ni/ZnO, only 40% conversion). On the other hand, at the same reaction time, a conversion of 50% was observed for Cu/ZnAl (with Cu/ZnO, 30%). The authors described the presence

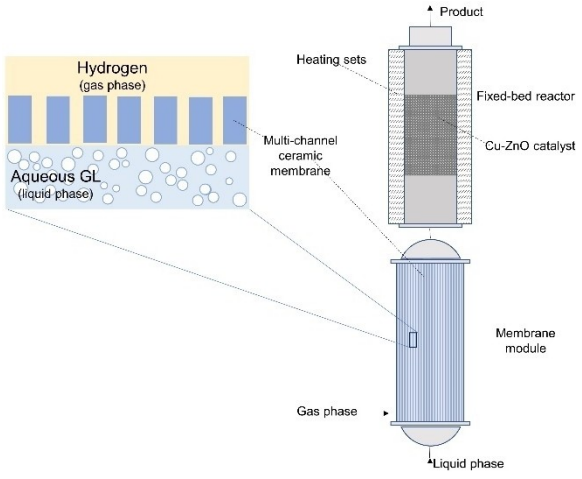

Figure 3. The fixed-bed reactor with the membrane dispersion for the continuous heterogeneous catalytic hydrogenolysis of GL. Adapted with permission from *Ind. Eng. Chem. Res.* 2018, 57, 1, 158–168. Copyright 2018 American Chemical Society.

of a NiZn alloy as the suppressor of the small molecules formation (*i.e.*, methane) and the production of lactide as the main product (22% yield at 60% conversion) while, in the case of Cu supported on ZnAl and ZnO, HAc formation (29% and 26% respectively) was observed.[206]

Yfanti *et al.* carried out two reactions in parallel: the liquid phase GL HDO and the methanol reforming over a Cu:Zn:Al catalyst at 523 K.[207] As a result, under poor hydrogen conditions (methanol/GL low ratio), GL dehydrogenated following the glyceraldehyde route to 1,2-PD, which further slightly hydrodeoxygenated to 1-PO. The last one dehydrogenated back to HAc with high H_2 concentrations (methanol/GL high ratio).[208] In a Cu-Al-Zn system, consisting mainly of hydrotalcite, the presence of basic sites was found to be mandatory for the GL hydrogenation, and the copper species, in the reaction carried out without hydrogen, proved to be essential for increasing the 1,2-PD selectivity.[186]

A Cu-Zn-Mg-Al-O catalyst was also employed in the preparation of 1,2-PD, resulting active and selective when in presence of NaOH; unfortunately, this catalyst was not reusable because of the sintering of ZnO and Cu that deactivated it.[209] Several ZnPd nanoparticles supported on the Al-doped ZnO were also prepared by modifying the calcination temperature of the supports: increasing the temperature from 623 K to 1023 K, a clear reduction of the activity (GL conversion from 70 to 25% and 1,2-PD selectivity from 93 to 79%) was observed.[210]

PdZn alloy was supported on monoclinic ZrO_2 to catalyze GL hydrogenolysis in water solution obtaining 1,2-PD at 493 K and 60 bar H_2.[211] The kinetically and selectively relevant step on metal surfaces was the α-C–H cleavage in 2,3-dihydroxypropanoxide to glyceraldehyde (step 3, Scheme 12), the intermediate compound to form the 1,2-PD (Scheme 13). Zn showed higher oxophilicity than Pd promoting the abstraction of α-H atom synergistically by adjacent Pd site.[211]

The authors calculated ΔG of the C–H cleavage: in presence of the PdZn alloys, it was lower than the value for Pd alone by 17 kJ mol^{-1}.

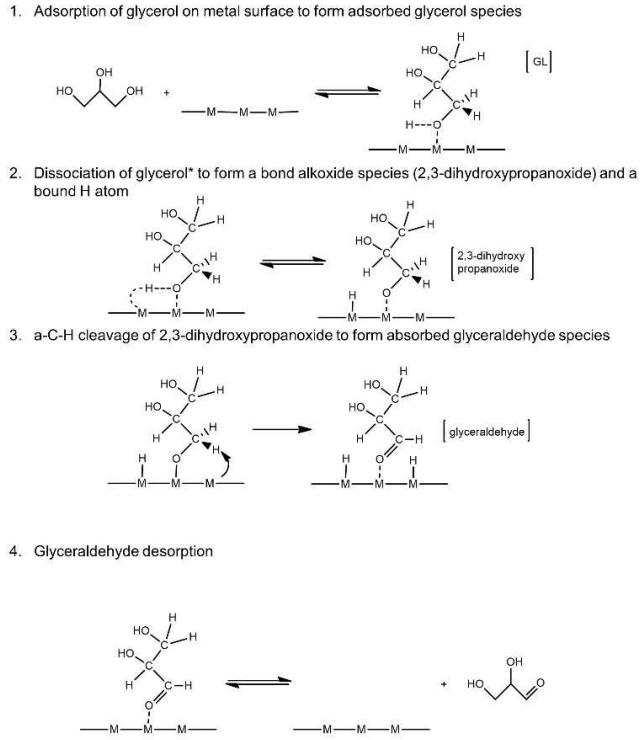

Scheme 12. Proposed steps for the hydrogenolysis of GL on metal surface to glyceraldehyde. Adapted with permission from Q. Sun, S. Wang, H. Liu, *ACS Catal.* 2017, 7, 4265–4275. Copyright 2017 American Chemical Society.

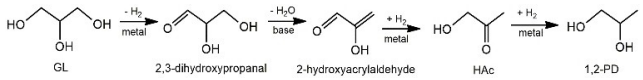

Scheme 13. Full metal catalyzed pathway of GL hydrogenolysis to 1,2-PD in aqueous solution. Adapted with permission from Q. Sun, S. Wang, H. Liu, *ACS Catal.* 2017, 7, 4265–4275. Copyright 2017 American Chemical Society.

3.6. Ruthenium

Despite its relatively expensive nature (average market price: 15,140 $/kg),[212] ruthenium is widely used in catalysis and for industrial purposes because of its high activity. Freshly prepared $Ru/Mg(OH)_2$ catalyst showed the best catalytic activity in the GL hydrogenolysis compared to commercial $Ru/Mg(OH)_2$ or Ru/MgO (synthesized or commercial): the synthesized catalyst containing $Mg(OH)_2$ displayed a cotton-like morphology; Ru was highly dispersed on the support and strong basic active sites were present, leading 1,2-PD with 65% selectivity and 24% GL conversion at 483 K and 30 bar H_2 pressure.[213] Poor results were observed in the presence of catalyst containing commercial $Mg(OH)_2$: 6% conversion and 57% selectivity of 1,2-PD.[213] Mane *et al.* underlined the correlation between the selectivity in GL hydrogenolysis and the precursor used to synthesize the catalyst: Ru/C catalyst prepared from $RuCl_3{\cdot}3H_2O$ showed high activity in C–C cleavage (ethylene glycol selectivity 56% and 1,2-PD 23%) while, in the case of $Ru(NO)(NO_3)_3$ precursor, low conversion (< 30%) but higher selectivity to 1,2-PD (44%) and lower to ethylene glycol (42%) were observed at 450–510 K and 52 H_2 bar.[214] By reducing the Ru catalysts in the presence of H_2 rather than with $NaBH_4$, the C–C cleavage products were suppressed and only C_3 compounds were obtained. In this case, both the reaction conditions and the reaction method to prepare the catalyst influenced the properties (texture, active surface area, acidity) of the catalyst itself.[214] Employing Ru–WO_x/C, it was possible to use milder temperature and pressure of the hydrogenolysis (423 K and 5 bar) with 73% conversion and quantitative 1,2-PD selectivity because the Ru nanoparticles activity was tuned by the acidity of the WO_x species at Ru/W molar ratio = 4.[215]

Ru-Mo catalyst supported on carbon nanotubes was used in the presence of phosphotungstic acid at 473 K and 60 H_2 bar.[216] 1,2-PD was produced with 53% selectivity (51% conversion): the presence of Mo oxides promoted the selective adsorption of the secondary -OH of GL and the phosphotungstic acid helped the initial dehydration.[216] The same group

prepared Ru-Mo supported on active carbon modified by phosphotungstic acid: at 40 bar and 473 K, the main products were 1,2-PD (74% selectivity) and 1,3-PD (21%).[217]

The addition of copper to Ru nanoparticles, dispersed on multiwall carbon nanotubes by wet impregnation, significantly affected the reducibility of the metallic species, promoting the C–O cleavage.[218] The conversion was limited (18%) but a remarkable 1,2-PD selectivity (93%), at 473 K and 50 H_2 bar, was obtained.[218] Recently, Pd-Ru nanoparticles were supported on a series of metal oxides and zeolitic supports with the aim of understanding the correlation between the catalytic activity (conversion and 1,2-PD yield) and the support acidity.[219] It was observed that C_3 products (instead of C_2 and C_1) were favored at 20 bar H_2 and 438 K, using catalysts displaying a moderate density of strong acid sites (130 NH_3 μmol g^{-1} on 230 NH_3 mmol g^{-1} of total acidity) as in TiO_2, giving 55% GL conversion and 1,2-PD with 50% selectivity.[219] Significative differences using Ru or Ru-Cu modified-zirconia catalysts were found in the hydrogenolysis at 453 K and 25 bar H_2: the Ru-based converted 30% of the aqueous GL (1,2-PD selectivity 60%) and the Ru-Cu transformed only 14% but with a very high selectivity (89%).[220] The superficial presence of copper (added on surface after ruthenium) addressed the reaction towards the C–O cleavage protecting the C–C bond from the Ru action.[221]

A series of Ru, Os, Pd, Cu catalysts supported on fluorine-doped tin oxide were tested towards the formation of 1,2-PD: as a result, Ru-based catalyst displayed the best activity at 423 K, with a 94% selectivity and a full conversion of GL, under 20 bar H_2.[222]

3.7. Palladium

Pd is a TM used more in the GL oxidation than its reduction, nevertheless, some articles are present in the literature about this topic (Pd average market price: 41,000 $/kg).[223] Rosas *et al.* compared LaY and Pd/LaY catalysts (with HY zeolite) in the dehydration reaction of GL.[224] The most active catalyst was Pd/LaY getting 90% GL conversion and leading to Acr and HAc as main products. The presence of small amounts of Pd on the surface of the catalyst positively promoted the elimination of coke precursors as a result of the reduction reactions in the presence of H_2 at atmospheric pressure. The conversion of GL increased with the raise in temperature as well as the acid sites concentration, leading Acr in 95% yield at 573 K.[224] Even Pd and PdO nanoparticles (3.8 nm) supported on SBA-15 were able to dehydrate GL to Acr (64% selectivity with 90% conversion) at 593 K and 2 bar in a continuous fixed-bed reactor.[225] The activity of the catalyst was maintained up to 20 h and after, gradually, its catalytic sites were deactivated by metal sintering and carbon depositions.

Pd nanoparticles were loaded into sulfate-functionalized metal-organic frameworks for hydrogenolysis purposes, obtaining a moderate conversion of GL (24%) with full selectivity for 1,2-PD.[226] This catalyst contained BAS, on the sulfate species of metal-organic frameworks, useful for dehydration step, as well as the Pd for the dehydrogenation step.

Pd species, in a PtPd on activated carbon, were responsible of the activity of the catalyst in the hydrogenolysis at 473 K and 10 N_2 bar (1,2-PD selectivity: 45%).[227] The results were due to the strong interactions between metal and support promoting the formation of Pd carbide that influenced the electronic arrangement of Pt.[227]

Hydrogenolysis of GL to 1-PO and 2-PO was performed at vapor phase in a fixed-bed reactor by using bifunctional 1–4 wt% Pd/MoO_3-Al_2O_3 catalyst prepared by wetness impregnation method.[228] The synergic interaction between the Pd and MoO_3 on Al_2O_3 support and its weak-moderate acidity were the key factors determining its catalytic activity. At 483 K and 1 bar H_2 pressure, 2 wt% Pd/MoO_3-Al_2O_3 catalyst was the most active, with 88% GL conversion and 91% selectivity to propanols.[228]

3.8. Silver

Only few and early works were reported in literature using silver as catalyst for GL conversion (Ag powder average market price: 887.16 $/kg).[229] Lari *et al.* deposited Ag nanoparticles onto a hierarchical ZSM-5 zeolite, to create a bifunctional catalyst to be employed in the gas phase GL dehydration–hydrogenation to AA *via* Acr using a continuous fixed-bed reactor.[230] The role of silver was to reduce the Acr into AA (selectivity 20%) in the presence of H_2. Furthermore, the activity of Ag degraded the coke deposited over the solid prolonging the life of the catalyst.

3.9. Iridium

Iridium, as noble metal (its average market price: 188,360 $/kg),[231] is able to activate the H_2, keeping its metallic properties; therefore monometallic and multimetallic metal species, combined with acidic components, were frequently used in the preparation of metal–acid bifunctional catalysts for the hydrogenolysis of GL to 1,2- and 1,3-PD (Scheme 14, pathway 3).[232]

1,3-PD was produced when using ReO_x-Ir/SiO_2 as catalyst, and then transformed in 1-PO by a successive dehydroxylation

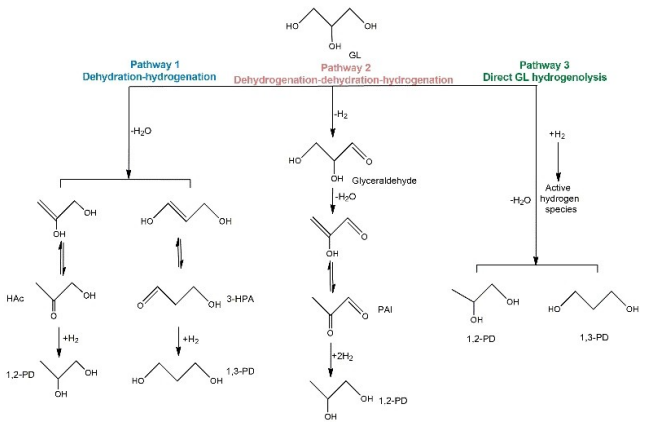

Scheme 14. Proposed mechanisms of GL hydrogenolysis to produce propanediols.

pathway, due to partially reduced ReO_x clusters, finely dispersed and directly interacting with the metallic Ir nanoparticles. In the highly concentrated GL solution, it was possible to achieve 50% reagent conversion thanks to more favorable substrate-catalyst interactions. However, the same result could be obtained by adding sulfuric acid in the reaction mixture because it increased GL amount within the silica pores, favoring the dissociation of GL to a primary propoxide. Therefore, working at 393 K with an initial hydrogen pressure of 80 bar, the selectivities were: 35% 1,3-PD, 18% 1,2-PD, 32% 1-PO, and 10% 2-PO.[127] Recently, 1,3-PD selectivity was related to Ir amount in bimetallic catalyst Ir/ReO_x: higher Ir loading amount (20 wt%) was, lower ratio of Re/Ir was, more active the catalyst was, leading to 1,3-PD in 32% yield, with a 47% selectivity and 69% GL conversion, at 80 bar H_2 and 393 K.[233] It was pointed out that the absence of Ir-Re alloy and the presence of ReO_x clusters at low valence attached to metallic Ir were responsible for this outcome.[234]

HZSM-5 was also reported as support for Ir-based catalysts involved in dehydrogenation of GL. Wan *et al.* prepared it *via* grinding-assisted impregnation method and attempted it as an effective and recyclable catalyst for the aqueous-phase hydrogenolysis of GL to 1,3-PD (75% selectivity at 453 K and 80 H_2 bar) in the absence of acid additives.[235] Ir dispersions, proper Ir^0/Ir^{3+} ratios and, more importantly, the amounts of overall acid/Brönsted acid sites seemed to influence reactivity and selectivity. To achieve good results, the size of IrO_x particles should be small (1.7 nm) and the Ir^0/Ir^{3+} ratio should be 40/60.[235] Moreover, the use of rutile TiO_2 as support for Ir-ReO_x led to a reasonable yield of 1,3-PD (36%): indeed, a high density of Ir particles over the TiO_2 surface, covered with the ReO_x cluster, resulted in highly active Ir-ReO_x interface.[30]

An attractive and safer method to carry out the reaction of GL deoxygenation is to generate H_2 *in situ*. The addition of Pt in the Ir-ReO_x/SiO_2 catalyst (0.5 wt%) led to the formation of two main active sites for C–O hydrogenolysis: Pt-Ir alloy and Ir-ReO_x species were able to catalyze aqueous phase reforming at 463 K, providing 81% GL conversion with 56% HAc and 19% 1,2-PD selectivity without external hydrogen sources.[233] The addition of Fe to Ir/TiO_2 (rutile) catalyzed the formation of 1,2-PD (selectivity, 67% at full GL conversion) after 42 h at 453 K and 80 H_2 bar and the overhydrogenolysis to propanols after 144 h (about 30% selectivity both 1-PO and 2-PO).[236] The active catalyst was constituted by the interface between Ir-Fe alloy and FeO_x species.

3.10. Platinum

Pt is a noble metal (its average market price: 32,535,700 $/kg)[237] mainly useful in the hydrogenolysis of GL.[238] The effects of several pore sizes of Pt/WO_x/Al_2O_3 catalyst was studied in the hydrogenolysis reaction.[239] The littlest pores (6 nm *vs.* 40 nm) resulted in superior Pt dispersion (32% *vs.* 29%), smaller metal crystallite size (3.5 nm *vs.* 3.9 nm) and a great number of active metallic sites (0.47 mmol NH_3 g^{-1} *vs.* 0.32 mmol NH_3 g^{-1}); but the diffusional constraint within pore channels inhibited the transport of reactant and product, lowering one third GL conversion and 1,3-PD yield.[239] Using a catalyst with the same metal loading but with large pores, 1,3-PD was obtained in a 33% yield from aqueous GL (78% conversion) at 493 K, 60 H_2 bar, after 5 h reaction.[239] The catalyst was proposed as bifunctional active site, formed by closely interacting Pt species, that activated the hydrogen, and $W^{\delta+}$-O-Al sites, necessary for the adsorption and activation of GL.[240] Good results in the production of 1,3-PD were obtained even in the presence of Pt-WO_x/α-Al_2O_3 calcinated at high temperature.[241] Its preparation method allowed to disperse Pt as single atom on solid surface, with more Pt and WO_x interactions. Therefore, the catalytic efficiency (conversion of 60% and selectivity of 44% for 1,3-PD and 27% for 1-PO), obtained at 453 K, 50 H_2 bar for 24 h, was attributed to the *in situ* generated BAS due to the strong interactions between the isolated WO_4 species and Pt.[241] The deactivation of this catalyst, however, seems to be due to the aggregation of Pt particles during the reactions,[242] that could be prevented by Re addition.[243] The temperatures of preparation are crucial: calcining WO_x/Al_2O_3 at 1073 K, WO_x species were connected to form W-O-W clusters and, after the Pt impregnation, a new calcination was conducted at 873 K and, then, the catalyst was reduced at 723 K.[244]

As seen, the combination of Pt and W is successful for the formation of 1,3-PD. García-Fernández *et al.* prepared Pt/WO_x/γ-Al_2O_3 catalysts to elucidate the role of Al and W species to bind GL terminal OH groups.[245] Employing *in situ* and *ex situ* ATR-IR spectroscopy, it was demonstrated that the bond with W resulted to be the strongest one, leading to a 38% yield of 1,3-PD at 473 K, 45 bar of H_2 and after 4 h reaction.[245] The presence of an oxophilic metal, as W, together with Pt, acted as an anchoring site for the terminal hydroxyl groups of GL and protonating the secondary hydroxyl group, leading to the formation of 1,3-PD as main product.[245] The optimum Pt/W atomic ratio was reported around 1/2-1/4.[246] The hydrogenolysis of aqueous GL was carried out in a fixed-bed down-flow stainless steel reactor at 453 K and 50 bar, obtaining 80% GL conversion and 1,3-PD in 28% yield (35% selectivity) in the presence of 6Pt/12.9 W/Al_2O_3. Hydrogen spillover occurred in the easy to reduce WO_x domains thanks to the presence of very well dispersed Pt species.[246] Pt single atoms on tungsten oxide were accredited as greatly stabilized when trapped into hollow site near WO_x(001) region and negatively charged, to favor the H_2 homolytic cleavage to metal-H species, as demonstrated by both DFT studies and experimental results.[106] The creation of Pt-H onto the support caused the formation of BAS, essential to the 1,3-PD selectivity.[106] Even the texture of support (Al_2O_3) resulted to be critical for the performance of the Pt/WO_x/Al_2O_3 catalysts. Two-dimensional nanosheets with an open pore structure turned out to have the best morphology of alumina for hydrogenolysis to 1,3-PD in comparison with the rod- or the spindle-shaped structures.[247] A bifunctional Pt-WO_3 supported TiP (titanium phosphate) catalyst was used to obtain 1,3-PD (51% selectivity at 85% of conversion) at 483 K and room pressure in a fixed-bed quartz reactor thanks to the strong interactions between Pt and WO_3 species and to the high number of BAS.[248]

W and Al were incorporated in SBA-15 using it as support for Pt nanoparticles.[249] The catalyst displayed synergistic and equilibrated BAS and LAS, contributing to relevant GL conversion (66%) and 1,3-PD selectivity (50%) at 60 bar H_2 and 433 K after 12 h reaction. The 64% conversion and 57% 1,3-PD selectivity were reported with Pt-WO_x/SiO_2 at 433 K and under 80 bar of H_2.[250] The high catalytic efficiency originated from the strong Brönsted acidity, due to the appropriate polymerization degree of WO_x and to its synergism with Pt metal. As DFT studies underlined, medium polymeric WO_x domains (dimeric HW_2O_7 cluster can delocalize more negative charge to the wider Pt surface, leading to a much stronger BAS), with no reduction of catalyst, showed the strongest Brönsted acidity and the lowest apparent activation energy in the formation of 1,3-PD. The importance of strong BAS evidenced that, in these conditions, the hydrodeoxygenation mechanism was involved in the 1,3-PD formation.[250]

Recently, 1,3-PD 63% was reported as yield at 423 K under 40 bar H_2 pressure, in the presence of a tungsten-doped siliceous mesostructured cellular foams-supported Pt catalyst (Pt/W-1.5MCFs).[251] Pt species gave spillover hydrogen atoms to W^V on the interface between the Pt nanoparticles and the W-MCFs. This peculiarity, combined with the particular 3D catalyst structure, was the explanation for the good results of these W-MCFs.[251]

In order to maximize the Pt-O-W interface with well dispersed Pt, low-polymeric WO_x on the Ta_2O_5 surface were reported as support for Pt: a thin layer of the WO_x-Ta_2O_5 solid solution on the Ta_2O_5 surface was obtained by calcinating the catalyst at 1173 K, leading to 48% GL conversion and 1,3-PD 40% selectivity, at 50 H_2 bar and 333 K after 12 h reaction.[252]

Several studies focused on the properties and the activity of the Pt-WO_x deposited on Zr solid supports as catalysts for GL hydrogenolysis.[253–255] Pt-WO_X was deposited on two different crystal phases of ZrO_2: when tetragonal ZrO_2 was used, the Pt particles size was smaller (0.59 nm *vs.* 0.72 nm) and the number of BAS higher than in the case of monoclinic phase.[254] These aspects drove the hydrogenolysis toward 49% 1,3-PD yield and 80% conversion at 413 K and 80 bar H_2 pressure (the values with monoclinic catalyst were cut in half).[254]

By an easy deposition method, Pt was incorporated onto preformed Au/WO_3 catalyst, to study the effect of gold as doping agent in Pt/WO_x catalyst.[256] Even in this case, several effects (*e.g.*, Pt well dispersed and in low-valence state, assistance in the redox cycle) for selective hydrogenolysis of GL to 1,3-PD led to 54% selectivity but lower GL conversion (30%) at 50 bar and 453 K.[256]

Wen *et al.* studied the effect of Ru in the Pt/WO_x/Al_2O_3 catalyst for GL hydrogenolysis.[257] 2Pt-1Ru/WO_x/Al_2O_3 catalyst afforded a 90% GL conversion, compared to 2Pt/WO_x/Al_2O_3 catalyst (70% GL conversion), with 40% selectivity for 1,3-PD, when performing the reaction at 90 bar and 443 K. Ru addition and its interaction with Pt species could restrain the condensation of metals preventing the growth of the nanoparticle sizes. Moreover, Ru was able to promote the redox cycle of tungsten and to increase the adsorption of hydrogen.[257]

Using the coimpregnation-calcination method, the Pt–1$Li_2B_4O_7$/WO_x/ZrO_2 was prepared modifying Pt/WO_x/ZrO_2 with $Li_2B_4O_7$.[258] This catalyst showed increased activity and stability (200 h) during the hydrogenolysis of GL due to good Pt dispersion and high BAS. Hydrogenolysis of GL was carried out at 423 K and 40 H_2 bar in a fixed-bed stainless steel reactor where the catalyst was put in the center of the reaction tube and fixed with quartz sand at both ends. After 100 h, a high conversion of 91% and a 45% yield of 1,3-PD were obtained.[258]

Even by changing the structural characteristic of support, *i.e.* using ordered mesoporous alumina instead of the commonly used γ-Al_2O_3 in the synthesis of PtNPs-HSiW/Al_2O_3, it was possible to increase Pt dispersion (from 15 to 35%) and the Brønsted acidity (from 12 to 30 μmol/g).[259]

The structural modifications influenced 1,3-PD production, doubling it. Therefore, working at 473 K and 40 H_2 bar in batch reactor, the GL conversion and the 1,3-PD selectivity were 60% and 33% respectively; in the recycle runs, the catalyst retained its activity despite the leaching.[259]

WO_3-Al_2O_3-SiO_2 was indicated as active support for Pt nanoparticles: it was synthesized by sol–gel method followed by Pt deposition for impregnation.[260] The catalyst showed high selectivity for 1,3-PD, around 56%, on 48% GL conversion in batch reactor, at 60 H_2 bar and 433 K. The authors presented a potential mechanism *via* acid-catalyzed dehydration and following hydrogenation on metal sites (Scheme 15).[260]

62% of 1,3-PD selectivity and 94% GL conversion were obtained in vapor phase, using sulfuric acid-activated montmorillonite clay as support for 2 wt% Pt nanoparticles, at 473 K, 1 H_2 bar in a fixed-bed reactor.[261] The good selectivity was due to the presence of strong BAS, coming from the acid activation of the support.

Von-Held Soares *et al.* compared Pt, Pd and Ni supported on Fe_3O_4 in the GL hydrogenolysis to 1,2-PD at 493 K.[262] The activity order for the tested catalysts was Pt > Pd > Ni, directly

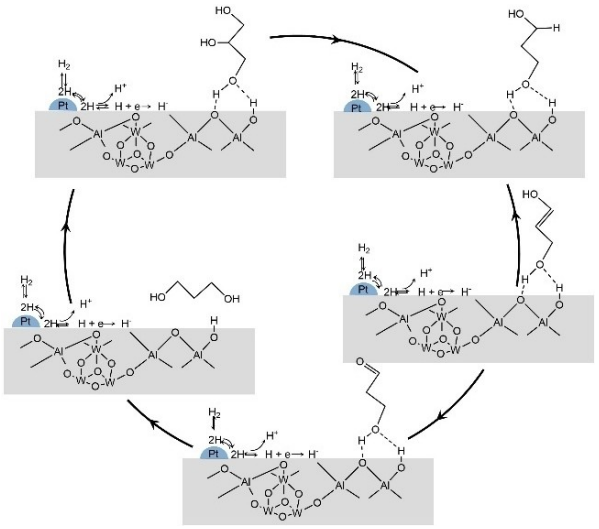

Scheme 15. Proposed mechanism of the 1,3-PD preparation over Pt on WO_3-Al_2O_3-SiO_2. Adapted from S. Feng, B. Zhao, L. Liu, J. Dong, *Ind. Eng. Chem. Res.* 2017, 56, 11065–11074. Copyright 2017 American Chemical Society.

related to the stability of the reduced nanoparticles. The main advantage of Fe_3O_4-supported catalysts was their easy removal from the reaction mixture by using a magnet, that can facilitate their potential reuse and recycle. In the reactions with Pt catalyst, the conversion was 81% and the selectivity to 1,2-PD was 79% (HAc 6% and 1-PO 5%).[262] The interactions between the metal and the FeO_x support were studied to find the appropriate catalyst to transform GL into 1,3-PD (78% selectivity) in the absence of H_2 at 513 K.[263] It was important that the catalyst, 2.5%Pt/FeO_x, was reduced at 473 K to form electron-rich Pt near the oxygen vacancy and the iron cation ($Pt^{\delta-}$-O_V-Fe^{2+}) that were the active sites.[263]

Significant results of GL HDO (83% conversion) and 1,2-PD selectivity (43%) were reported, also without H_2, using trimetallic 2%Ru-2%Re-2% Pt/C catalyst and MgO as solid base promoter, carrying out the reaction at 493 K and under 20 N_2 bar.[264]

In the past, the hydrogenolysis was proposed in presence of a base to facilitate the dehydrogenation steps to 1,2-PD; recently, a theoretical and experimental study about the very positive effect of alkaline earth metal cations with Pt/C in the GL reaction was published.[265]

Considering that the hydrogenolysis of the GL (to diols) with metal/Al_2O_3 is essentially driven by the interaction between the acid sites of alumina and the metal species, Du *et al.* introduced a method to increase the metal-acid interface making the catalyst more active.[266] The authors synthesized porous Al_2O_3 coating onto a Pt/Al_2O_3 catalyst using atomic layer deposition. The catalyst promoted 90% GL conversion, leading to 1,2-PD with 64% selectivity at 493 K and a pressure of H_2 of 80 bar.[266]

The dimension of metal nanoparticles is critical for the catalysis: the size of Pt nanoparticles influenced the reaction mechanism and, consequently, the selectivity of the products. For example, using 2% Pt/Al_2O_3, it was possible to tune the products varying the nanoparticles size, from 1,2-PD (with 3–4 nm Pt) to hydrogen gas (with 2 nm Pt).[267] Pt nanoparticles of 2 nm, but supported on a CeO_2 modified with ZrO_2, were used to catalyze the HDO at 443 K and 10 bar H_2 obtaining 1,2-PD selectively (74%).[268]

Zhang *et al.* published GL hydrogenolysis by Pt-In alloy catalyst, prepared by impregnation of indium and platinum precursors onto the MgAl support, followed by calcination and reduction process.[269] At 473 K and 20 H_2 bar, the authors obtained full GL conversion and a remarkable selectivity for 1,2-PD (91%). The active site was established as $Pt^{\delta-}$ for adsorbing GL through the primary C–O and breaking the appropriate terminal C–H bond, preserving the C–C bond.[269]

Sulfates-doped Pt-WO_x/TiO_2 catalyst achieved 100% conversion of GL, with 36% selectivity to 1,3-PD and 57% selectivity to 1-PO at 393 K and 40 bar.[270] Its activity, higher than the no-doped catalyst, was ascribed not only to the better dispersion of Pt and WO_x species and more BAS, but also to its stability due to the action of sulfate in the redox cycle, and then in the prevention of leaching of both Pt and WO_x species.

Amorphous zirconium phosphate-supported Pt catalyst was modified with the incorporation of WO_x, with the purpose of enhancing the acidity (mainly LAS) and the dispersion of Pt nanoparticles.[271] In particular, in the presence of Pt/7WO_x-ZrP catalyst, 81% yield of 1-PO at full conversion of GL in a continuous-flow fixed-bed reactor at 543 K and 20 H_2 bar was obtained. This catalyst showed stability for 70 h of reaction. Moreover, by calcination at air, it was possible to regenerate it obtaining an active catalyst for 50 h, with similar conversion and yield.[271] Similar propanol selectivity, by 34% conversion, was reported for a Pt onto Zr-Al mixed oxides (Pt/$Zr_{0.7}Al_{0.3}O_y$), with a >80% selectivity to 1-PO at 503 K and 60 bar H_2.[272]

3.11. Gold

The fascinating catalytic activity of gold (its average market price: 67,860 $/kg)[273] in coordination and organometallic chemistry has been attracting researchers for fifty years, as evidenced even in the reactions of deoxygenation of GL.[274]

A two-step synthesis of AAc from GL was proposed: in the first step, AA is produced by a formic acid catalyzed DODH reaction, while in the second step, after switching the pH from acidic to basic, the oxidation of AA to AAc occurred in the presence of Au/CeO_2 with 87% yield.[275] This cascade reaction was realized to overcome the difficulty of separation of AA from formic acid residue in the first step, due to their similar boiling points, while it is not difficult to separate AAc from formic acid by distillation (their boiling points are sufficiently different). The newly formed AAc can undergo hydration, side reaction that can be avoided using low reaction temperature (298 K), high oxygen pressure (10 bar) and a dilute AA concentration (0.1 M). Between the different shapes of CeO_2 tested (*e.g.*, rods, octahedra, cubes) as support, octahedra showed the best results and were very stable during recycling (up to the fifth run, 80% yield).[275] WO_x was proposed as support for AuPt-based catalysts: in the presence of AuPt/WO_x catalyst, 81% GL conversion and 52% 1,3-PD selectivity were obtained at 413 K, 10 bar H_2.[113] The presence of Au modified the structure of Pt/WO_x and provided more activated W species for the formation of frustrated Lewis-pair analogs, namely for more catalytic *in situ* generated BAS.[113]

When using Au-Pt/WO_x/Al_2O_3, at 453 K and 50 bar, the conversion of GL was 78% obtaining 1,3-PD with 55% selectivity.[276] The addition of small amounts of Au, that likely were present as single atoms and forming Au-WO_x clusters interacting with Pt, diminished the strong metal support interactions between Pt and WO_x sites. Platinum species were more exposed and active in the H-spillover and, therefore, in the formation of strong BAS. The good performance only slightly decreased, reusing the catalyst (fourth run: 1,3-PD selectivity 56%).[276] AuPt/TiO_2 proved to be more active than AuPt/MCM41, AuPt/SiO_2, AuPt/H-mordenite, AuPt/sulfated ZrO_2 in the formation of 1,2-PD (selectivity 90% at 68%conversion of GL), while AuPt/MgO worked very well (selectivity >90%), but it deactivated quickly.[17] The superiority of AuPt/TiO_2 was due to the acid strength of the support, related in inverse proportion to catalysts activity; also the small size (4 nm) of Au nanoparticles was essential.[17]

4. Conclusions and future perspectives

As just seen in the previous sections, several catalytic routes to convert the GL into useful C_3 compounds can be proposed to the industrial world, reaching out also the Sustainable Development Goals by United Nations.[277]

To better understand which metals are more suitable for obtaining safer, cheaper, and widely diffused low polar C_3 derivatives, we explored the up-to-date published data, simply grouping TMs in: early (from Sc to Mn group) and late (from Fe to Zn group). In both Figures, 4 and 5, we reported the number of articles (art), obtained from a scientific database, using, as research keys, the name of each metal associated to each single C_3 derivative and to GL in the time range 2017–2023.

It is not immediate to rationalize the reports since, for example, they involve both the use of metal as real catalyst and as support, or systems with a synergic catalytic effect between them.

Even considering what has just been said, the use of Cu to obtain 1,2-PD represents the most studied process (242 art) and, furthermore, 1,2-PD is the C_3 chemical reported in the largest number of studies (926 art, of which 173 with early and 753 with late metals). An overview on the total number of art highlights how their number, per single metal (average value), is clearly in favor of late TMs (early: 859 art / 9 TMs = 95.44; late: 1864 art / 11 TMs = 169.45). The traditional explanation for this difference is the strong resistance of early TMs to undergo redox cycling because of their weak electronegativity (*e.g.*, 1.4 for Sc *vs* 1.9 for Cu).[278] Nevertheless, we can affirm that, apart from Fe, which is the most abundant TM found on the Earth's crust (51,000 g/ton),[279] the other most abundant metals are represented on the early region (Ti, 6,300 g/ton; Mn, 930 g/ton; Cr, 200 g/ton; Zr, 190 g/ton),[279] and, furthermore, they are endowed of a relatively low toxicity. These two last considerations suggest that, probably, the catalytic studies involving the less toxic and more abundant early TMs, to obtain low oxygenated derivatives from natural wastes, must be increased and that the actual gap in scientific literature is a chance, and not a limitation, to develop innovative and, above all, sustainable catalytic technologies.

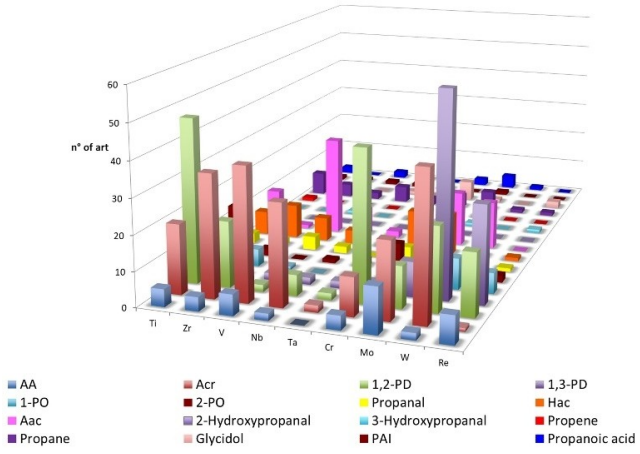

Figure 4. Number of papers in literature of early TMs as catalysts for the deoxygenation of GL to C_3 compounds.

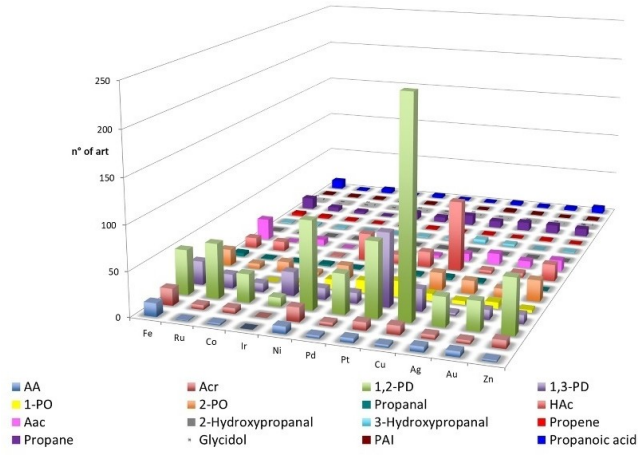

Figure 5. Number of papers in literature of late TMs as catalysts for the deoxygenation of GL to C_3 compounds.

In our research group, for several years, selective deoxygenation studies on natural polyols have been carried out using an early TM (*i.e.*, rhenium),[10,125,129,133,280] which can be, in our opinion, a starting point for moving to analogous (from the catalytic point of view) metals, such as Mo or V.[281–284]

However, efficient deoxygenation performance is not solely determined by the choice of the metal catalyst. As strongly demonstrated by this review, the actual applications mainly employ traditional thermochemical methodologies to transform polyols to low-oxygenated, carbon-equivalent, chemicals.

From the literature, the alternative energy-suppliers, *e.g.* photochemistry, mechanochemistry or electrochemistry, were scarcely utilized.

Marcì *et al.* obtained Acr irradiating, with UV light, a water suspension of GL and Keggin heteropolyacids supported on TiO_2.[285] This one example demonstrates that photochemistry can be a feasible alternative to conventional productions of fine and commodity chemicals. Several TM catalysts, described in previous sections, like Keggin heteropolyacids, WO_x or TiO_2, are photoactive and could be used, in the future, as photocatalysts to deoxygenate the GL.[286]

It is worth noticing that in some cases, composite catalysts could be prepared by solid-state grinding, leading to mesoporous composites where the precursors species were introduced into the channels of the mesoporous material, with an improved interaction between the metal precursors and the silica template (removed after calcination of the catalyst). In most of the cases, catalysts prepared by (manual) grinding showed a high BET surface area compared to the traditional methods, which results, generally speaking, in catalytic system outperforming confronted to those prepared by conventional solvent-based methods. However, to the best of our knowledge, deoxygenation of GL to access C_3 compounds activated by grinding or by milling remains unexplored, the only and still very few, examples being limited to the preparation of the catalysts needed for the reaction. The reasons behind this gap might be due to the difficulties in accessing dedicated milling devices to handle gases under pressure, other than the lack of

cross-fertilization of knowledge. Therefore, it could be expected that, in the future, these limitations will be overcome and new process conditions, based on mechanical activation, will be disclosed for GL deoxygenation to value-add C_3 chemicals.[287] Examples of preparation of C_3 chemicals from GL also include activation by ultrasounds.[288]

Even electrochemical synthetic methods represent a valid alternative to provide energy in the deoxygenations. The delay in the use of such technology may be due to several reasons: i) a suitable electrochemical device is necessary and its cost and maintenance are not particularly cheap; ii) to promote an efficient electron transfer in solution, an electrolyte usually must be introduced together with a solvent that can be not particularly green (toluene, THF, etc.).[289]

The knowledge gained so far about the metal catalysts must prompt us to deeply explore the TMs world, which is not fully understood, to improve, even with the use of alternative energies, the transformations of waste polyols to fine chemicals without carbon loss.

List of Abbreviations

1-PO	Propane-1-ol
2-PO	Propane-2-ol
1,2-PD	Propane-1,2-diol
1,3-PD	Propane-1,3-diol
3-HPA	3-Hydroxypropanal
AA	Allyl alcohol
AAc	Acrylic acid
Acr	Acrolein
art	Articles
BAS	Brønsted acid site
DODH	Deoxydehydration
DFT	Density functional theory
GL	Glycerol
HAc	Hydroxyacetone
HDO	Hydrodeoxygenation
LAS	Lewis acid site
MTO	Methyltrioxorhenium
PAl	Pyruvaldehyde
PAAH	Polyacrylic acid
SAA	Single atom alloy
TM	Transition metal

Acknowledgements

The research project was partially supported by the FSE-REACT-EU, PON Ricerca e Innovazione 2014-2020 DM 1062/2021, Cod: MUR 53-G-14753.

Conflict of Interests

The authors declare no conflict of interest.

Keywords: glycerol · hydrogenation · early transition metal · late transition metal · catalysis · deoxygenation

[1] D. Novembre, D. Gimeno, N. d'Alessandro, L. Tonucci, *Mineral. Mag.* **2018**, *82*, 961–973.
[2] B. Roozbehani, M. Mirdrikvand, S. I. Moqadam, A. C. Roshan, *Chem. Technol. Fuels Oils* **2013**, *49*, 115–124.
[3] A. Mohsenzadeh, A. Zamani, M. J. Taherzadeh, *ChemBioEng Rev.* **2017**, *4*, 75–91.
[4] Z. Kong, L. He, Y. Shi, Q. Guan, P. Ning, *Heliyon* **2020**, *6*, e03446.
[5] A. Chatterjee, S. H. Hopen Eliasson, V. R. Jensen, *Catal. Sci. Technol.* **2018**, *8*, 1487–1499.
[6] K. C. Kwon, H. Mayfield, T. Marolla, B. Nichols, M. Mashburn, *Renewable Energy* **2011**, *36*, 907–915.
[7] S. Dutta, *ChemSusChem* **2020**, *13*, 2894–2915.
[8] M. Stalpaert, K. Janssens, C. Marquez, M. Henrion, A. L. Bugaev, A. V Soldatov, D. De Vos, *ACS Catal.* **2020**, *10*, 9401–9409.
[9] N. N. Tshibalonza, J.-C. M. Monbaliu, *Green Chem.* **2020**, *22*, 4801–4848.
[10] V. Canale, L. Tonucci, M. Bressan, N. D'Alessandro, *Catal. Sci. Technol.* **2014**, *4*, 3697–3704.
[11] M. McCoy, *Chem. Eng. News* **2012**, *90*.
[12] T. Attarbachi, M. D. Kingsley, V. Spallina, *Fuel* **2023**, *340*, 127485.
[13] A. Franciosini, M. Molica Colella, G. Anweta, M. Costagliola, *Glycerol to Biofuel: Market, Technologies and Players* **2022**.
[14] "Titanium Market Price," can be found under https://www.metal.com/Titanium/201211080001, **2023**.
[15] P. Sudarsanam, H. Li, T. V. Sagar, *ACS Catal.* **2020**, *10*, 9555–9584.
[16] S. N. Delgado, D. Yap, L. Vivier, C. Especel, *J. Mol. Catal. A* **2013**, *367*, 89–98.
[17] A. Villa, M. Manzoli, F. Vindigni, L. E. Chinchilla, G. A. Botton, L. Prati, *Catal. Lett.* **2017**, *147*, 2523–2533.
[18] R. Mane, Y. Jeon, C. Rode, *Green Chem.* **2022**, *24*, 6751–6781.
[19] M. R. Md Radzi, M. D. Manogaran, M. H. M. Yusoff, Zulqarnain, M. R. Anuar, N. F. Shoparwe, M. F. A. Rahman, *Catalysts* **2022**, *12*, 945.
[20] Z. Xi, W. Jia, Z. Zhu, *Catal. Lett.* **2020**, *151*, 124–137.
[21] Y. Zeng, L. Jiang, X. Zhang, S. Xie, Y. Pei, G. Zhou, W. Hua, M. Qiao, Z. H. Li, B. Zong, *ACS Sustainable Chem. Eng.* **2022**, *10*, 9532–9545.
[22] Y. Chen, Y. Zeng, C.-T. Hung, Z. Zhang, Z. Lv, S. Huang, Y. Yang, Y. Liu, W. Li, *Nano Res.* **2023**, *16*, 9081–9090.
[23] Z. Luo, Z. Zhu, R. Xiao, D. Chu, *Chem. Asian J.* **2022**, *18*, e202201046.
[24] A. Żelazny, K. Samson, R. Grabowski, M. Śliwa, M. Ruggiero-Mikołajczyk, A. Kornas, *React. Kinet. Mech. Catal.* **2017**, *121*, 329–343.
[25] B. C. M. Morales, B. A. O. Quesada, *Catal. Today* **2021**, *372*, 115–125.
[26] S. Ginjupalli, P. Balla, H. Shaik, N. Nekkala, B. Ponnala, H. Mitta, *New J. Chem.* **2019**, *43*, 16860–16869.
[27] Z. Babaei, A. Najafi Chermahini, M. Dinari, *J. Colloid Interface Sci.* **2020**, *563*, 1–7.
[28] E. Kraleva, H. Atia, *React. Kinet. Mech. Catal.* **2019**, *126*, 103–117.
[29] P. Bhanuchander, S. S. Priya, V. P. Kumar, S. Hussain, N. Pethan Rajan, S. K. Bhargava, K. V. R. Chary, *Catal. Lett.* **2017**, *147*, 845–855.
[30] L. Liu, T. Asano, Y. Nakagawa, M. Tamura, K. Okumura, K. Tomishige, *ACS Catal.* **2019**, *9*, 10913–10930.
[31] "Vanadium Market Price," can be found under https://www.metal.com/Other-Minor-Metals/201102250299, **2023**.
[32] F. A. Cotton, G. Wilkinson, C. A. Murillo, M. Bochmann, *Advanced Inorganic Chemistry, 6th Edition* **1999**.
[33] R. R. Langeslay, D. M. Kaphan, C. L. Marshall, P. C. Stair, A. P. Sattelberger, M. Delferro, *Chem. Rev.* **2019**, *119*, 2128–2191.
[34] J. L. Dubois, C. Duquenne, *Ep 1 853 713 B1* **2012**.
[35] G. Licini, V. Conte, A. Coletti, M. Mba, C. Zonta, *Coord. Chem. Rev.* **2011**, *255*, 2345–2357.
[36] D. Liu, B. Chen, J. Li, Z. Lin, P. Li, N. Zhen, Y. Chi, C. Hu, *Inorg. Chem.* **2021**, *60*, 3909–3916.
[37] D. Brown, in *Encycl. Toxicol.*, Elsevier, **2014**, pp. 74–75.
[38] A. Chieregato, C. Bandinelli, P. Concepción, M. D. Soriano, F. Puzzo, F. Basile, F. Cavani, J. M. L. Nieto, *ChemSusChem* **2017**, *10*, 234–244.
[39] D. Sun, Y. Yamada, S. Sato, W. Ueda, *Green Chem.* **2017**, *19*, 3186–3213.
[40] M. Y. Ahmad, N. I. Basir, A. Z. Abdullah, *J. Ind. Eng. Chem.* **2021**, *93*, 216–227.
[41] L. G. Possato, M. D. Acevedo, C. L. Padró, V. Briois, A. R. Passos, S. H. Pulcinelli, C. V. Santilli, L. Martins, *J. Mol. Catal.* **2020**, *481*, 110158.
[42] F. A. Bezerra, H. O. N. Altino, R. R. Soares, *J. Braz. Chem. Soc.* **2019**, *30*, 1025–1033.

[43] B. Viswanadham, V. Vishwanathan, K. V. R. Chary, Y. Satyanarayana, *J. Porous Mater.* **2021**, *28*, 1269–1279.
[44] L. F. Rasteiro, L. H. Vieira, C. V. Santilli, L. Martins, *RSC Adv.* **2018**, *8*, 11975–11982.
[45] L. H. Vieira, A. Lopez-Castillo, C. W. Jones, L. Martins, *Appl. Catal. A* **2020**, *602*, 117687.
[46] A. R. Petersen, L. B. Nielsen, J. R. Dethlefsen, P. Fristrup, *ChemCatChem* **2018**, *10*, 769–778.
[47] H. S. Oliveira, P. P. Souza, L. C. A. Oliveira, *Catal. Today* **2017**, *289*, 258–263.
[48] R. Almeida, M. F. Ribeiro, A. Fernandes, J. P. Lourenço, *Catal. Commun.* **2019**, *127*, 20–24.
[49] A. Fernandes, M. F. Ribeiro, J. P. Lourenço, *Microporous Mesoporous Mater.* **2022**, *329*, 111536.
[50] A. Abdullah, M. Ahmed, D. V. N. Vo, A. Z. Abdullah, *Waste Biomass Valorization* **2023**, *15*, 163–175.
[51] H. Lan, Q. Yao, Y. Zhou, B. Zhang, Y. Jiang, *J. Mol. Catal.* **2020**, *498*, 111279.
[52] "Chromium Market Price," can be found under https://www.metal.com/Chromium/201102250234, **2023**.
[53] M. Sperling, in *Encycl. Anal. Sci.*, Elsevier, **2005**, pp. 113–126.
[54] US EPA, Priority Pollutant List, https://www.epa.gov/sites/default/files/2015-09/documents/priority-pollutant-list-epa.pdf **2014**.
[55] Y. S. Yun, T. Y. Kim, D. Yun, K. R. Lee, J. W. Han, J. Yi, *ChemSusChem* **2017**, *10*, 442–454.
[56] R. A. Luizon Filho, L. G. Possato, O. A. N. Santisteban, A. de Vasconcellos, D. A. da Silva, M. F. Lima, L. Martins, J. G. Nery, *Inorg. Chem. Commun.* **2020**, *112*, 107710.
[57] R. Munirathinam, J. Huskens, W. Verboom, *Adv. Synth. Catal.* **2015**, *357*, 1093–1123.
[58] F. P. Kinik, S. Kampouri, F. M. Ebrahim, B. Valizadeh, K. C. Stylianou, *2.30 - Porous Metal-Organic Frameworks for Advanced Applications*, Editor(s): Edwin C. Constable, Gerard Parkin, Lawrence Que Jr, Comprehensive Coordination Chemistry III, Elsevier, **2021**, 590–616.
[59] "Zirconium Market Price," can be found under https://www.metal.com/Other-Minor-Metals/201102250232, **2023**.
[60] F. Cai, X. Song, Y. Wu, J. Zhang, G. Xiao, *ACS Sustainable Chem. Eng.* **2018**, *6*, 110–118.
[61] R. Luo, X. Zhao, H. Gong, W. Qian, D. Li, M. Chen, K. Cui, J. Wang, Z. Hou, *Energy Fuels* **2020**, *34*, 8707–8717.
[62] G. Srinivasa Rao, S. Hussain, K. V. R. Chary, *Mater. Today: Proc.* **2018**, *5*, 25773–25781.
[63] H. Gong, C. Zhou, Y. Cui, S. Dai, X. Zhao, R. Luo, P. An, H. Li, H. Wang, Z. Hou, *ChemSusChem* **2020**, *13*, 4954–4966.
[64] T. Leungcharoenwattana, S. Jitkarnka, *Chem. Eng. Trans.* **2019**, *76*, 109–114.
[65] "Niobium Market Price," can be found under https://www.metal.com/Niobium-Tantalum/201102250606, **2023**.
[66] S. M. A. H. Siddiki, M. N. Rashed, M. A. Ali, T. Toyao, P. Hirunsit, M. Ehara, K. ichi Shimizu, *ChemCatChem* **2019**, *11*, 383–396.
[67] M. Tarselli, *Nat. Chem.* **2015**, *7*, 180.
[68] N. La Salvia, D. Delgado, L. Ruiz-Rodríguez, L. Nadji, A. Massó, J. M. L. Nieto, *Catal. Today* **2017**, *296*, 2–9.
[69] D. Delgado, A. Fernández-Arroyo, M. E. Domine, E. García-González, J. M. López Nieto, *Catal. Sci. Technol.* **2019**, *9*, 3126–3136.
[70] D. Delgado, P. Concepción, A. Trunschke, J. M. López Nieto, *Dalton Trans.* **2020**, *49*, 13282–13293.
[71] K. H. Sung, S. Cheng, *RSC Adv.* **2017**, *7*, 41880–41888.
[72] C. García-Sancho, J. A. Cecilia, J. M. Mérida-Robles, J. Santamaría González, R. Moreno-Tost, A. Infantes-Molina, P. Maireles-Torres, *Appl. Catal. B* **2018**, *221*, 158–168.
[73] C. F. M. Pestana, B. P. Pinto, D. R. Fernandes, C. J. A. Mota, *J. Braz. Chem. Soc.* **2022**, *33*, 1154–1162.
[74] K. Stawicka, M. Trejda, M. Ziolek, *Catalysts* **2021**, *11*, 488.
[75] S. Jeon, Y. M. Park, J. Park, K. Saravanan, H. K. Jeong, J. W. Bae, *Appl. Catal. A* **2018**, *551*, 49–62.
[76] F. Cai, F. Jin, J. Hao, G. Xiao, *Catal. Commun.* **2019**, *131*, 105801.
[77] M. Yang, X. Zhao, Y. Ren, J. Wang, N. Lei, A. Wang, T. Zhang, *Cuihua Xuebao/Chinese J. Catal.* **2018**, *39*, 1027–1037.
[78] H. S. Oliveira, J. M. Resende, P. P. Souza, P. S. O. Patrício, L. C. A. Oliveira, *J. Braz. Chem. Soc.* **2017**, *28*, 2244–2253.
[79] "Molybdenum Market Price," can be found under https://www.metal.com/Other-Minor-Metals/201102250481, **2023**.
[80] V. M. L. Whiffen, K. J. Smith, *Energy Fuels* **2010**, *24*, 4728–4737.
[81] A. Kostyniuk, D. Bajec, P. Djinović, B. Likozar, *Chem. Eng. J.* **2020**, *397*, 125430.
[82] H. Lan, J. Zeng, B. Zhang, Y. Jiang, *Res. Chem. Intermed.* **2019**, *45*, 1565–1580.
[83] W. Wan, S. C. Ammal, Z. Lin, K. E. You, A. Heyden, J. G. Chen, *Nat. Commun.* **2018**, *9*, 1–10.
[84] A. D. Anderson, M. P. Lanci, J. S. Buchanan, J. A. Dumesic, G. W. Huber, *ChemCatChem* **2021**, *13*, 425–437.
[85] H. Lan, X. Xiao, S. Yuan, B. Zhang, G. Zhou, Y. Jiang, *Catal. Lett.* **2017**, *147*, 2187–2199.
[86] V. Zacharopoulou, E. S. Vasiliadou, A. A. Lemonidou, *ChemSusChem* **2018**, *11*, 264–275.
[87] Z. Wu, H. Yan, S. Ge, J. Gao, T. Dou, Y. Li, A. C. K. Yip, M. Zhang, *Catal. Commun.* **2017**, *92*, 80–85.
[88] M. Checa, V. Montes, J. Hidalgo-Carrillo, A. Marinas, F. Urbano, *Nanomaterials* **2019**, *9*, 509.
[89] M. Rellán-Piñeiro, N. López, *ACS Sustainable Chem. Eng.* **2018**, *6*, 16169–16178.
[90] G. Ioannidou, V.-Loukia Yfanti, A. A. Lemonidou, *Catal. Today* **2023**, *23*, 113902.
[91] X. Ren, F. Zhang, M. Sudhakar, N. Wang, J. Dai, L. Liu, *Catal. Today* **2019**, *332*, 20–27.
[92] S. T. Wu, Q. M. She, R. Tesser, M. Di Serio, C. H. Zhou, *Catal. Rev. Sci. Eng.* **2020**, *62*, 481–523.
[93] L. F. Rasteiro, L. H. Vieira, L. G. Possato, S. H. Pulcinelli, C. V. Santilli, L. Martins, *Catal. Today* **2017**, *296*, 10–18.
[94] L. G. Possato, M. D. Acevedo, C. L. Padró, V. Briois, A. R. Passos, S. H. Pulcinelli, C. V. Santilli, L. Martins, *Mol. Catal.* **2020**, *481*, 110158.
[95] S. Suganuma, T. Hisazumi, K. Taruya, E. Tsuji, N. Katada, *J. Mol. Catal.* **2018**, *449*, 85–92.
[96] "Tantalum Market Price," can be found under https://www.metal.com/Niobium-Tantalum/202107020003, **2023**.
[97] S. Natarajan, V. Gopalan, R. A. A. Rajan, C. P. Jen, *Materials (Basel).* **2021**, *14*, 1660.
[98] Z.-L. Xue, T. M. Cook, *4.10 - Tantalum*, Editor(s): Edwin C. Constable, Gerard Parkin, Lawrence Que Jr, Comprehensive Coordination Chemistry III, Elsevier, **2021**, 375–445.
[99] B. Zhao, Y. Liang, L. Liu, Q. He, J. Dong, *Green Chem.* **2020**, *22*, 8254–8259.
[100] J. Wang, X. Zhao, N. Lei, L. Li, L. Zhang, S. Xu, S. Miao, X. Pan, A. Wang, T. Zhang, *ChemSusChem* **2016**, *9*, 784–790.
[101] K. Bhaduri, A. Ghosh, A. Auroux, S. Chatterjee, A. Bhaumik, B. Chowdhury, *J. Mol. Catal.* **2022**, *518*, 112074.
[102] "Tungsten Market Price," can be found under https://www.metal.com/Tungsten/201308090022, **2023**.
[103] F. Wu, H. Jiang, X. Zhu, R. Lu, L. Shi, F. Lu, *ChemSusChem* **2021**, *14*, 569–581.
[104] S. García-Fernández, I. Gandarias, Y. Tejido-Núñez, J. Requies, P. L. Arias, *ChemCatChem* **2017**, *9*, 4508–4519.
[105] C. Chen, Y. Liang, Q. Tang, D. Li, L. Liu, J. Dong, *Ind. Eng. Chem. Res.* **2022**, *61*, 12504–12512.
[106] M. Zhou, M. Yang, X. Yang, X. Zhao, L. Sun, W. Deng, A. Wang, J. Li, T. Zhang, *Chin. J. Catal.* **2020**, *41*, 524–532.
[107] G. Shi, Z. Cao, J. Xu, K. Jin, Y. Bao, S. Xu, *Catal. Lett.* **2018**, *148*, 2304–2314.
[108] W. Zhou, J. Luo, Y. Wang, J. Liu, Y. Zhao, S. Wang, X. Ma, *Appl. Catal. B* **2019**, *242*, 410–421.
[109] S. Bhowmik, N. Enjamuri, G. Sethia, V. Akula, B. Marimuthu, S. Darbha, *J. Mol. Catal.* **2022**, *531*, 112704.
[110] C. Wang, C. Chen, *React. Kinet. Mech. Catal.* **2019**, *128*, 461–477.
[111] Y. Niu, B. Zhao, Y. Liang, L. Liu, J. Dong, *Ind. Eng. Chem. Res.* **2020**, *59*, 7389–7397.
[112] L. Liu, T. Asano, Y. Nakagawa, M. Gu, C. Li, M. Tamura, K. Tomishige, *Appl. Catal. B* **2021**, *292*, 120164.
[113] X. Zhao, J. Wang, M. Yang, N. Lei, L. Li, B. Hou, S. Miao, X. Pan, A. Wang, T. Zhang, *ChemSusChem* **2017**, *10*, 819–824.
[114] A. A. Greish, E. D. Finashina, O. P. Tkachenko, P. A. Nikul'shin, M. A. Ershov, L. M. Kustov, *Mendeleev Commun.* **2020**, *30*, 119–120.
[115] C. T. Q. Mai, Y. Ye, G. L. Rempel, F. T. T. Ng, *Catal. Today* **2023**, *407*, 2–10.
[116] C. Hulteberg, A. Leveau, J. G. M. Brandin, *Top. Catal.* **2017**, *60*, 1462–1472.
[117] L. Nadji, A. Massó, D. Delgado, R. Issaadi, E. Rodriguez-Aguado, E. Rodriguez-Castellón, J. M. López Nieto, *RSC Adv.* **2018**, *8*, 13344–13352.

[118] Q. Xie, S. Li, R. Gong, G. Zheng, Y. Wang, P. Xu, Y. Duan, S. Yu, M. Lu, W. Ji, Y. Nie, J. Ji, *Appl. Catal. B* **2019**, *243*, 455–462.
[119] Y. Zengin, B. Kaya, M. Safak Boroglu, I. Boz, *Ind. Eng. Chem. Res.* **2023**, *62*, 1852–1864.
[120] T. Aihara, K. Asazuma, H. Miura, T. Shishido, *RSC Adv.* **2020**, *10*, 37538–37544.
[121] Z. Wang, L. Liu, *Catal. Today* **2021**, *376*, 55–64.
[122] D. Delgado, A. Chieregato, M. D. Soriano, E. Rodríguez-Aguado, L. Ruiz-Rodríguez, E. Rodríguez-Castellón, J. M. López Nieto, *Eur. J. Inorg. Chem.* **2018**, *2018*, 1204–1211.
[123] "Rhenium Market Price," can be found under https://www.metal.com/Other-Minor-Metals/201102250036, **2023**.
[124] C. P. Casey, *Science* **1993**, *259*, 1552–1558.
[125] V. Canale, A. Zavras, G. N. Khairallah, N. D'Alessandro, R. A. J. O'Hair, *Eur. J. Mass Spectrom.* **2015**, *21*, 557–567.
[126] M. L. Shozi, V. D. B. C. Dasireddy, S. Singh, P. Mohlala, D. J. Morgan, S. Iqbal, H. B. Friedrich, *Sustain. Energy Fuels* **2017**, *1*, 1437–1445.
[127] J. J. Varghese, L. Cao, C. Robertson, Y. Yang, L. F. Gladden, A. A. Lapkin, S. H. Mushrif, *ACS Catal.* **2019**, *9*, 485–503.
[128] S. Chanklang, W. Mondach, P. Somchuea, T. Witoon, M. Chareonpanich, K. Faungnawakij, A. Seubsai, *Catal. Today* **2022**, *397–399*, 356–364.
[129] M. Lupacchini, A. Mascitti, V. Canale, L. Tonucci, E. Colacino, M. Passacantando, A. Marrone, N. D'Alessandro, *Catal. Sci. Technol.* **2019**, *9*, 3036–3046.
[130] Y. Kon, M. Araque, T. Nakashima, S. Paul, F. Dumeignil, B. Katryniok, *ChemistrySelect* **2017**, *2*, 9864–9868.
[131] K. S. Vargas, J. Zaffran, M. Araque, M. Sadakane, B. Katryniok, *J. Mol. Catal.* **2023**, *535*, 112856.
[132] J. Li, M. Lutz, M. Otte, R. J. M. Klein Gebbink, *ChemCatChem* **2018**, *10*, 4755–4760.
[133] A. Mascitti, G. Scioli, L. Tonucci, V. Canale, R. Germani, P. Di Profio, N. D'Alessandro, *ACS Omega* **2022**, *7*, 27980–27990.
[134] "Iron Market Price," can be found under https://www.metal.com/Pig-Iron/202203070001, **2023**.
[135] M. B. dos Santos, H. M. C. Andrade, A. J. S. Mascarenhas, *Microporous Mesoporous Mater.* **2019**, *278*, 366–377.
[136] S. Lopez-Pedrajas, R. Estevez, J. Schnee, E. M. Gaigneaux, D. Luna, F. M. Bautista, *J. Mol. Catal.* **2018**, *455*, 68–77.
[137] T. Ma, J. Ding, X. Liu, G. Chen, J. Zheng, *Korean J. Chem. Eng.* **2020**, *37*, 955–960.
[138] M. M. Diallo, S. Laforge, Y. Pouilloux, J. Mijoin, *Catal. Lett.* **2018**, *148*, 2283–2303.
[139] M. M. Diallo, S. Laforge, Y. Pouilloux, J. Mijoin, *Catal. Commun.* **2019**, *126*, 21–25.
[140] N. Martín, M. D. L. Rodríguez, D. Solís-Casados, M. Viniegra, *J. Mex. Chem. Soc.* **2020**, *64*, 327–338.
[141] H. Fujitsuka, K. Terai, M. Hayashi, T. Yoshikawa, Y. Nakasaka, T. Masuda, T. Tago, *J. Jpn. Pet. Inst.* **2019**, *62*, 319–328.
[142] V. L. Yfanti, E. S. Vasiliadou, S. Sklari, A. A. Lemonidou, *J. Chem. Technol. Biotechnol.* **2017**, *92*, 2236–2245.
[143] G. Zhang, X. Jin, J. Wang, M. Liu, W. Zhang, Y. Gao, X. Luo, Q. Zhang, J. Shen, C. Yang, *Ind. Eng. Chem. Res.* **2020**, *59*, 17387–17398.
[144] H. Zhao, Y. Jiang, H. Liu, Y. Long, Z. Wang, Z. Hou, *Appl. Catal. B* **2020**, *277*, 119187.
[145] "Cobalt Market Price," can be found under https://www.metal.com/Cobalt/201102250186, **2023**.
[146] S. Lopez-Pedrajas, R. Estevez, J. Schnee, E. M. Gaigneaux, D. Luna, F. M. Bautista, *J. Mol. Catal.* **2018**, *455*, 68–77.
[147] S. Lopez-Pedrajas, R. Estevez, F. Blanco-Bonilla, D. Luna, F. M. Bautista, *J. Chem. Technol. Biotechnol.* **2017**, *92*, 2661–2672.
[148] N. Raju, V. Rekha, B. Abhishek, P. M. Kumar, C. Sumana, N. Lingaiah, *New J. Chem.* **2020**, *44*, 3122–3128.
[149] C. Sepúlveda, K. Cruces, J. Gajardo, J. Seguel, R. García, D. Salinas, J. L. G. Fierro, I. T. Ghampson, R. Serpell, N. Escalona, *New J. Chem.* **2019**, *43*, 15636–15645.
[150] F. Cai, Y. Guo, G. Xiao, *Chem. Eng. Technol.* **2023**, *46*, 256–263.
[151] H. Gong, X. Zhao, X. Li, M. Chen, Y. Ma, J. Fang, X. Wei, Q. Peng, Z. Hou, *ACS Sustainable Chem. Eng.* **2021**, *9*, 2246–2259.
[152] A. Lähde, R. J. Chimentão, T. Karhunen, M. G. Álvarez, J. Llorca, F. Medina, J. Jokiniemi, L. B. Modesto-López, *Adv. Powder Technol.* **2017**, *28*, 3296–3306.
[153] "Nickel Market Price," can be found under https://www.metal.com/Nickel/202008270001, **2023**.
[154] A. Syuhada, M. Ameen, M. Tazli, A. Aqsha, M. Hizami, M. Yusoff, A. Ramli, M. Sahban, F. Sher, *J. Mol. Catal.* **2021**, *514*, 111860–111876.
[155] A. Kant, Y. He, A. Jawad, X. Li, F. Rezaei, J. D. Smith, A. A. Rownaghi, *Chem. Eng. J.* **2017**, *317*, 1–8.
[156] C. T. Q. Mai, F. T. T. Ng, *Catal. Today* **2017**, *291*, 195–203.
[157] I. C. Freitas, R. L. Manfro, M. M. V. M. Souza, *Appl. Catal. B* **2018**, *220*, 31–41.
[158] T. S. de Andrade, M. M. V. M. Souza, R. L. Manfro, *Renewable Energy* **2020**, *160*, 919–930.
[159] D. K. Pandey, N. N. Pandhare, P. Biswas, *React. Kinet. Mech. Catal.* **2019**, *127*, 523–542.
[160] V. Rekha, N. Raju, C. Sumana, N. Lingaiah, *Catal. Lett.* **2017**, *147*, 1441–1452.
[161] M. L. Shozi, V. D. B. C. Dasireddy, S. Singh, A. Govender, P. Mohlala, H. B. Friedrich, *Sustain. Energy Fuels* **2019**, *3*, 2038–2047.
[162] Y. Yan, Y. Zhang, T. Jiang, T. Xiao, P. P. Edwards, F. Cao, *RSC Adv.* **2017**, *7*, 38251–38256.
[163] W. Long, F. Hao, W. Xiong, P. Liu, H. Luo, *React. Kinet. Mech. Catal.* **2017**, *122*, 85–100.
[164] M. N. Gatti, M. D. Mizrahi, J. M. Ramallo-Lopez, F. Pompeo, G. F. Santori, N. N. Nichio, *Appl. Catal. A* **2017**, *548*, 24–32.
[165] A. Ramesh, B. M. Ali, R. Manigandan, C. T. Da, M. T. Nguyen-Le, *J. Mol. Catal.* **2022**, *525*, 112358.
[166] F. Cai, D. Pan, J. J. Ibrahim, J. Zhang, G. Xiao, *Appl. Catal. A* **2018**, *564*, 172–182.
[167] V. Georgescu, C. Panaitescu, M. Bombos, D. Bombos, *Rev. Chim.* **2017**, *68*, 1114–1117.
[168] T. Hu, Z. Yu, S. Liu, B. Liu, Z. Sun, Y.-Y. Liu, A. Wang, Y. Wang, *New J. Chem.* **2021**, *45*, 21725–21731.
[169] M. N. Gatti, J. L. Cerioni, F. Pompeo, G. F. Santori, N. N. Nichio, *Catalysts* **2020**, *10*, 1–15.
[170] M. N. Gatti, M. D. Mizrahi, J. M. Ramallo-Lopez, F. Pompeo, G. F. Santori, N. N. Nichio, *Catal. Today* **2021**, *372*, 136–145.
[171] A. A. Greish, E. D. Finashina, O. P. Tkachenko, L. M. Kustov, *Molecules* **2021**, *26*, 1–16.
[172] Q. Han, J. Ge, Y. Yang, B. Liu, *React. Kinet. Mech. Catal.* **2019**, *127*, 331–343.
[173] "Copper Market Price," can be found under https://www.metal.com/Copper-Scrap/201108090019, **2023**.
[174] D. L. Manuale, L. V. Santiago, G. C. Torres, J. H. Sepúlveda, P. A. Torresi, C. R. Vera, J. C. Yori, *J. Chem. Technol. Biotechnol.* **2018**, *93*, 1050–1064.
[175] S. Mondal, H. Malviya, P. Biswas, *React. Chem. Eng.* **2019**, *4*, 595–609.
[176] G. S. Dmitriev, V. I. Khadzhiev, S. A. Nikolaev, D. I. Ezzhelenko, I. S. Mel'chakov, L. N. Zanaveskin, *Pet. Chem.* **2020**, *60*, 1066–1072.
[177] A. Bouriakova, P. S. F. Mendes, B. Katryniok, J. De Clercq, J. W. Thybaut, *Catal. Commun.* **2020**, *146*, 106134.
[178] S. A. Nikolaev, G. S. Dmitriev, K. L. Zanaveskin, T. B. Egorova, S. N. Khadzhiev, *Pet. Chem.* **2017**, *57*, 1074–1080.
[179] F. Vila, M. López Granados, R. Mariscal, *Catal. Sci. Technol.* **2017**, *7*, 3119–3127.
[180] P. Kumar, R. Kaur, S. Verma, U. L. Štangar, *Appl. Clay Sci.* **2023**, *232*, 106762.
[181] S. Liu, Z. Yu, C. Lu, Y. Wang, F. Sun, Z. Sun, Y. Liu, C. Shi, A. Wang, *Fuel* **2023**, *334*, 126763.
[182] H. Mitta, N. Devunuri, J. Sunkari, S. Mutyala, P. Balla, V. Perupogu, *Catal. Today* **2021**, *375*, 204–215.
[183] R. J. Chimentão, P. Hirunsit, C. S. Torres, M. B. Ordoño, A. Urakawa, J. L. G. Fierro, D. Ruiz, *Catal. Today* **2021**, *367*, 58–70.
[184] J. Mazarío, J. A. Cecilia, E. Rodríguez-Castellón, M. E. Domine, *Appl. Catal. A* **2023**, *652*, 119029.
[185] J. Shan, H. Liu, K. Lu, S. Zhu, J. Li, J. Wang, W. Fan, *J. Catal.* **2020**, *383*, 13–23.
[186] N. K. Mishra, P. Kumar, V. C. Srivastava, U. L. Stangar, *J. Environ. Chem. Eng.* **2021**, *9*, 1–7.
[187] D. K. Pandey, P. Biswas, *React. Chem. Eng.* **2020**, *5*, 2221–2235.
[188] J. Mazarío, P. Concepción, M. Ventura, M. E. Domine, *J. Catal.* **2020**, *385*, 160–175.
[189] S. Célerier, S. Morisset, I. Batonneau-Gener, T. Belin, K. Younes, C. Batiot-Dupeyrat, *Appl. Catal. A* **2018**, *557*, 135–144.
[190] C. P. Fu, Q. M. She, R. Tesser, C. H. Zhou, *Catal. Sci. Technol.* **2022**, *12*, 6495–6506.
[191] L. Omar, N. Perret, S. Daniele, *Catalysts* **2021**, *11*, 516.
[192] L. Omar, T. Onfroy, S. Daniele, N. Perret, *ChemCatChem* **2023**, *15*, e202201297.
[193] X. Zhang, G. Cui, H. Feng, L. Chen, H. Wang, B. Wang, X. Zhang, L. Zheng, S. Hong, M. Wei, *Nat. Commun.* **2019**, *10*, 1–12.

[194] A. N. Ardila, M. A. Sánchez-Castillo, T. A. Zepeda, A. L. Villa, G. A. Fuentes, *Appl. Catal. B* **2017**, *219*, 658–671.
[195] A. N. Ardila, E. Arriola-Villaseñor, G. A. Fuentes, *ACS Omega* **2020**, *5*, 19497–19505.
[196] A. L. Folkard, M. D. Farahani, A. S. Mahomed, H. B. Friedrich, *ChemCatChem* **2022**, *14*, e202200602.
[197] "Zinc Market Price," can be found under https://www.metal.com/Zinc/201102250367, **2023**.
[198] K. Frolich, J. Kocík, J. Mück, J. Kolena, L. Skuhrovcová, *Mol. Catal.* **2022**, *533*, 112796.
[199] D. K. Pandey, P. Biswas, *New J. Chem.* **2019**, *43*, 10073–10086.
[200] A. Al Ameen, S. Mondal, S. M. Pudi, N. N. Pandhare, P. Biswas, *Energy Fuels* **2017**, *31*, 8521–8533.
[201] S. Mondal, A. A. Arifa, P. Biswas, *Catal. Lett.* **2017**, *147*, 2783–2798.
[202] M. Hou, H. Jiang, Y. Liu, C. Chen, W. Xing, R. Chen, *Ind. Eng. Chem. Res.* **2018**, *57*, 158–168.
[203] L. Zheng, X. Li, W. Du, D. Shi, W. Ning, X. Lu, Z. Hou, *Appl. Catal. B* **2017**, *203*, 146–153.
[204] D. Durán-Martín, M. L. Granados, J. L. G. Fierro, C. Pinel, R. Mariscal, *Top. Catal.* **2017**, *60*, 1062–1071.
[205] M. Hou, H. Jiang, Y. Liu, R. Chen, *React. Kinet. Mech. Catal.* **2017**, *122*, 1129–1143.
[206] R. J. Chimentão, B. C. Miranda, D. Ruiz, F. Gispert-Guirado, F. Medina, J. Llorca, J. B. O. Santos, *J. Energy Chem.* **2020**, *42*, 185–194.
[207] V. L. Yfanti, A. A. Lemonidou, *J. Catal.* **2018**, *368*, 98–111.
[208] V. L. Yfanti, A. A. Lemonidou, *J. Catal.* **2018**, *368*, 98–111.
[209] S. Mondal, R. Janardhan, M. L. Meena, P. Biswas, *J. Environ. Chem. Eng.* **2017**, *5*, 5695–5706.
[210] X. Li, Q. Wu, B. Zhang, C. Zhang, W. Lin, H. Cheng, F. Zhao, *Catal. Today* **2018**, *302*, 210–216.
[211] Q. Sun, S. Wang, H. Liu, *ACS Catal.* **2017**, *7*, 4265–4275.
[212] "Ruthenium Market Price," can be found under https://www.metal.com/Other-Precious-Metals/201102250083, **2023**.
[213] J. Liu, L. Ruan, J. Liao, A. Pei, K. Yang, L. Zhu, B. H. Chen, *New J. Chem.* **2020**, *44*, 16054–16061.
[214] R. B. Mane, S. T. Patil, H. Gurav, S. S. Rayalu, C. V. Rode, *ChemistrySelect* **2017**, *2*, 1734–1745.
[215] A. Bellè, K. Kusada, H. Kitagawa, A. Perosa, L. Castoldi, D. Polidoro, M. Selva, *Catal. Sci. Technol.* **2022**, *12*, 259–272.
[216] G. Cai, S. Zhou, F. Hao, W. Xiong, P. Liu, *Catal. Lett.* **2021**, *151*, 2075–2087.
[217] G. Cai, W. Xiong, S. Zhou, P. Liu, Y. Lv, F. Hao, H. Luo, C. Kong, *Chin. J. Chem. Eng.* **2022**, *51*, 199–215.
[218] M. Sherbi, A. Wesner, V. K. Wisniewski, A. Bukowski, H. Velichkova, B. Fiedler, J. Albert, *Catal. Sci. Technol.* **2021**, *11*, 6649–6653.
[219] S. Guadix-Montero, A. Santos-Hernandez, A. Folli, M. Sankar, *Philos. Trans. R. Soc. London* **2020**, *378*, 20200055.
[220] A. L. P. Salgado, F. C. Araújo, A. V. H. Soares, Y. Xing, F. B. Passos, *Appl. Catal. A* **2021**, *626*, 118359.
[221] M. H. M. Pires, F. B. Passos, Y. Xing, *Catal. Today* **2023**, *419*, 114161.
[222] W. Z. Samad, W. N. R. Wan Isahak, N. Hamzah, M. A. Yarmo, M. Rahimi Yusop, *Mater. Sci. Forum* **2017**, *888*, 496–502.
[223] "Palladium Market Price," can be found under https://www.metal.com/Other-Precious-Metals/201102250083, **2023**.
[224] I. P. Rosas, J. L. Contreras, J. Salmones, C. Tapia, B. Zeifert, J. Navarrete, T. Vázquez, D. C. García, *Catalysts* **2017**, *7*, 1–29.
[225] R. Pothu, N. Mameda, R. Boddula, H. Mitta, V. Perugopu, N. Al-Qahtani, *Mater. Sci. Energy Technol.* **2023**, *6*, 226–236.
[226] J. Zhang, Z. Li, X. He, Y. Cao, C. Wang, *New J. Chem.* **2021**, *45*, 21263–21269.
[227] D. Zhang, W. Yu, Z. Li, Z. Wang, B. Yin, X. Liu, J. Shen, C. Yang, W. Yan, X. Jin, *Biomass and Bioenergy* **2022**, *163*, 106507.
[228] S. P. Samudrala, *Catalysts* **2018**, *8*, 385.
[229] "Silver Market Price," can be found under https://www.metal.com/Other-Precious-Metals/201102250463, **2023**.
[230] G. M. Lari, Z. Chen, C. Mondelli, J. Pérez-Ramírez, *ChemCatChem* **2017**, *9*, 2195–2202.
[231] "Iridium Market Price," can be found under https://www.metal.com/Other-Precious-Metals/201102250587, **2023**.
[232] Y. Wang, J. Zhou, X. Guo, *RSC Adv.* **2015**, *5*, 74611–74628.
[233] S. Liu, M. Tamura, Z. Shen, Y. Zhang, Y. Nakagawa, K. Tomishige, *Catal. Today* **2018**, *303*, 106–116.
[234] L. Liu, S. Kawakami, Y. Nakagawa, M. Tamura, K. Tomishige, *Appl. Catal. B* **2019**, *256*, 117775–117788.
[235] X. Wan, Q. Zhang, M. Zhu, Y. Zhao, Y. Liu, C. Zhou, Y. Yang, Y. Cao, *J. Catal.* **2019**, *375*, 339–350.
[236] B. Liu, Y. Nakagawa, C. Li, M. Yabushita, K. Tomishige, *ACS Catal.* **2022**, *12*, 15431–15450.
[237] "Platinum Market Price," can be found under https://www.metal.com/Other-Precious-Metals/201102250529, **2023**.
[238] D. Zhang, Q. Zhang, Z. Zhou, Z. Li, K. Meng, T. Fang, Z. You, G. Zhang, B. Yin, J. Shen, C. Yang, W. Yan, X. Jin, *ChemCatChem* **2022**, *14*, e202101316.
[239] T. Numpilai, C. K. Cheng, A. Seubsai, K. Faungnawakij, J. Limtrakul, T. Witoon, *Environ. Pollut.* **2021**, *272*, 116029.
[240] C. Jarauta-Córdoba, M. Oregui Bengoechea, I. Agirrezabal-Telleria, P.-L. Arias, I. Gandarias, *Catalysts* **2021**, *11*, 1171.
[241] B. Zhao, Y. Liang, L. Liu, Q. He, J. X. Dong, *ChemCatChem* **2021**, *13*, 3695–3705.
[242] Y. Wen, S. Liu, W. Shen, Y. Fang, *Chem. Eng. Commun.* **2023**, *210*, 1291–1304.
[243] T. Saelee, T. Tapanya, C. Wangphon, M. Rittiruam, T. Miyake, P. Khemthong, T. Butburee, P. Limsoonthakul, S. Praserthdam, P. Praserthdam, *Fuel* **2022**, *326*, 125019.
[244] N. Dolsiririttigul, T. Numpilai, C. Wattanakit, A. Seubsai, K. Faungnawakij, C. K. Cheng, D. V. N. Vo, S. Nijpanich, N. Chanlek, T. Witoon, *Top. Catal.* **2023**, *66*, 205–222.
[245] S. García-Fernández, I. Gandarias, J. Requies, F. Soulimani, P. L. Arias, B. M. Weckhuysen, *Appl. Catal. B* **2017**, *204*, 260–272.
[246] N. Lei, X. Zhao, B. Hou, M. Yang, M. Zhou, F. Liu, A. Wang, T. Zhang, *ChemCatChem* **2019**, *11*, 3903–3912.
[247] W. Xu, P. Niu, H. Guo, L. Jia, D. Li, *React. Kinet. Mech. Catal.* **2021**, *133*, 173–189.
[248] B. Ponnala, P. Balla, S. K. Hussain, S. R. Ginjupalli, K. Koppadi, N. Nekkala, V. Perupogu, U. Lassi, P. K. Seelam, *Waste Biomass Valorization* **2022**, *13*, 4389–4402.
[249] S. Feng, B. Zhao, Y. Liang, L. Liu, J. Dong, *Ind. Eng. Chem. Res.* **2019**, *58*, 2661–2671.
[250] W. Zhou, Y. Li, X. Wang, D. Yao, Y. Wang, S. Huang, W. Li, Y. Zhao, S. Wang, X. Ma, *J. Catal.* **2020**, *388*, 154–163.
[251] S. Cheng, Y. Fan, X. Zhang, Y. Zeng, S. Xie, Y. Pei, G. Zeng, M. Qiao, B. Zong, *Appl. Catal. B* **2021**, *297*, 120428.
[252] B. Zhao, Y. Liang, W. Yan, L. Liu, J. Dong, *Ind. Eng. Chem. Res.* **2021**, *60*, 12534–12544.
[253] S. Bhowmik, N. Enjamuri, S. Darbha, *New J. Chem.* **2021**, *45*, 5013–5022.
[254] Y. Fan, S. Cheng, H. Wang, J. Tian, S. Xie, Y. Pei, M. Qiao, B. Zong, *Appl. Catal. B* **2017**, *217*, 331–341.
[255] W. Zhou, J. Luo, Y. Wang, J. Liu, Y. Zhao, S. Wang, X. Ma, *Appl. Catal. B* **2019**, *242*, 410–421.
[256] C. Yang, F. Zhang, N. Lei, M. Yang, F. Liu, Z. Miao, Y. Sun, X. Zhao, A. Wang, *Cuihua Xuebao/Chinese J. Catal.* **2018**, *39*, 1366–1372.
[257] Y. Wen, W. Shen, Y. Li, Y. Fang, *React. Kinet. Mech. Catal.* **2021**, *132*, 219–233.
[258] M. Zhu, C. Chen, *React. Kinet. Mech. Catal.* **2018**, *124*, 683–699.
[259] M. Gu, Z. Shen, L. Yang, B. Peng, W. Dong, W. Zhang, Y. Zhang, *Ind. Eng. Chem. Res.* **2017**, *56*, 13572–13581.
[260] S. Feng, B. Zhao, L. Liu, J. Dong, *Ind. Eng. Chem. Res.* **2017**, *56*, 11065–11074.
[261] S. S. Pryia, S. Kandasamy, S. Bhattacharya, *Sci. Rep.* **2018**, *8*, 7484.
[262] A. Von Held Soares, H. Atia, U. Armbruster, F. B. Passos, A. Martin, *Appl. Catal. A* **2017**, *548*, 179–190.
[263] G. Shu, Y. Lin, S. Wang, S. Zhang, L. Fan, C. Wang, C. Zhou, L. Song, L. Zheng, J. Zhang, K. Ma, H. Yue, *ACS Catal.* **2023**, *13*, 8423–8436.
[264] A. Torres, H. Shi, B. Subramaniam, R. V. Chaudhari, *ACS Sustainable Chem. Eng.* **2019**, *7*, 11323–11333.
[265] A. K. Beine, X. Wang, M. Vennewald, R. U. S. Schmidt, C. Glotzbach, R. Palkovits, P. J. C. Hausoul, *ChemCatChem* **2022**, *202101940*, e202101940.
[266] H. Du, S. Chen, H. Wang, J. Lu, *Cuihua Xuebao/Chinese J. Catal.* **2017**, *38*, 1237–1244.
[267] J. Callison, N. D. Subramanian, S. M. Rogers, A. Chutia, D. Gianolio, C. R. A. Catlow, P. P. Wells, N. Dimitratos, *Appl. Catal. B* **2018**, *238*, 618–628.
[268] E. A. Redina, K. V. Vikanova, O. P. Tkachenko, G. I. Kapustin, L. M. Kustov, *Dokl. Chem.* **2022**, *507*, 261–269.
[269] X. Zhang, G. Cui, M. Wei, *Ind. Eng. Chem. Res.* **2020**, *59*, 12999–13006.
[270] Z. Zhou, H. Jia, Y. Guo, Y. Wang, X. Liu, Q. Xia, X. Li, Y. Wang, *ChemCatChem* **2021**, *13*, 3953–3959.

[271] R. Luo, X. Zhao, H. Gong, W. Qian, D. Li, M. Chen, K. Cui, J. Wang, Z. Hou, *Energy Fuels* **2020**, *34*, 8707–8717.
[272] C. Li, B. He, Y. Ling, C. W. Tsang, C. Liang, *Cuihua Xuebao/Chinese J. Catal.* **2018**, *39*, 1121–1128.
[273] "Gold Market Price," can be found under https://www.metal.com/Gold/201102250531, **2023**.
[274] S. A. Shahzad, M. A. Sajid, Z. A. Khan, D. Canseco-Gonzalez, *Synth. Commun.* **2017**, *47*, 735–755.
[275] M. Kim, H. Lee, *ACS Sustainable Chem. Eng.* **2017**, *5*, 11371–11376.
[276] B. Wang, F. Liu, W. Guan, A. Wang, T. Zhang, *ACS Sustainable Chem. Eng.* **2021**, *9*, 5705–5715.
[277] UN General Assembly, *70/1. Transforming Our World: The 2030 Agenda for Sustainable Development* **2015**, https://www.un.org/en/development/desa/population/migration/generalassembly/docs/globalcompact/A RES 70 1 E.pdf.
[278] J. Guo, X. Deng, C. Song, Y. Lu, S. Qu, Y. Dang, Z. X. Wang, *Chem. Sci.* **2017**, *8*, 2413–2425.
[279] V. M. Goldschimdt, *J. Chem. Soc.* **1937**, 655–673.
[280] G. Scioli, L. Tonucci, P. Di Profio, A. Proto, R. Cucciniello, N. d'Alessandro, *Sustain. Chem. Pharm.* **2020**, *17*, 100273.
[281] E. Aksanoglu, Y. H. Lim, R. A. Bryce, *ChemSusChem* **2021**, *14*, 1545–1553.
[282] R. R. Langeslay, D. M. Kaphan, C. L. Marshall, P. C. Stair, A. P. Sattelberger, M. Delferro, *Chem. Rev.* **2019**, *119*, 2128–2191.
[283] F. C. Jentoft, *Catal. Sci. Technol.* **2022**, *12*, 6308–6358.
[284] A. R. Petersen, P. Fristrup, *Chem. A Eur. J.* **2017**, *23*, 10235–10243.
[285] G. Marcì, E. García-López, V. Vaiano, G. Sarno, D. Sannino, L. Palmisano, *Catal. Today* **2017**, *281*, 60–70.
[286] D. Cambié, T. Noël, *Top. Curr. Chem.* **2018**, *376*, 1–27.
[287] E. Colacino, V. Isoni, D. Crawford, F. García, *Trends Chem.* **2021**, *3*, 335–339.
[288] M. Lupacchini, A. Mascitti, G. Giachi, L. Tonucci, N. d'Alessandro, J. Martinez, E. Colacino, *Tetrahedron* **2017**, *73*, 609–653.
[289] Y. Yuan, A. Lei, *Nat. Commun.* **2020**, *11*, 2018–2020.

Manuscript received: December 18, 2023
Revised manuscript received: December 22, 2023
Accepted manuscript online: December 28, 2023
Version of record online: ■■, ■■

REVIEW

The large availability of glycerol could make convenient to deoxygenate it to obtain chemicals that can be used for applications such as energy, polymers, and fine chemistry. Transition metals are efficient catalysts to perform such transformations and here we explored the recent literature to understand which metals could represent the economical, green and effective candidates to transform glycerol into C_3 compounds, otherwise obtainable from fossil resource.

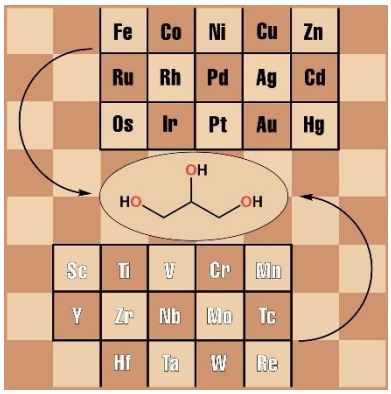

*Dr. F. Coccia, Prof. N. d'Alessandro, Dr. A. Mascitti, Prof. Dr. E. Colacino, Dr. L. Tonucci**